Marine Geology
January 2020, Volume 419, Pages 106064 (15p.)
https://doi.org/10.1016/j.margeo.2019.106064
https://archimer.ifremer.fr/doc/00588/70052/

Heat flow in the Western Mediterranean: Thermal anomalies on the margins, the seafloor and the transfer zones

Poort Jeffrey [1, *], Lucazeau Francis [2], Le Gal Virginie [1, 3], Dal Cin Michaela [4], Leroux Estelle [5], Bouzid Abderrezak [6], Rabineau Marina [7], Palomino Désirée [8], Battani Anne [3], Akhmanov G. Grigory [9], Ferrante G. Matilde [4], Gafurova R. Dina [9], Si Bachir Roza [6], Koptev Alexander [1], Tremblin Maxime [1], Bellucci Massimo [7], Pellen Romain [5], Camerlenghi Angelonghi [4], Migeon Sebastien [10], Alonso Belen [11], Ercilla Gemma [11], Yelles-Chaouche A. Karim [6], Khlystov M. Oleg [12]

[1] Sorbonne Université, CNRS, Institut des Sciences de la Terre de Paris, ISTeP, Paris, France
[2] Université de Paris, Institut de Physique du Globe de Paris, CNRS, Paris, France
[3] IFP Energies nouvelles, Geosciences, Rueil-Malmaison, France
[4] Istituto Nazionale di Oceanografia e di Geofisica Sperimentale (OGS), Trieste, Italy
[5] IFREMER, 1625 Route de Sainte-Anne, 29280 Plouzané, France
[6] Centre de Recherche en Astronomie Astrophysique et Géophysique (CRAAG), Alger, Algeria
[7] Institut Universitaire Européen de la Mer (IUEM), Université de Bretagne Occidentale, Laboratoire Domaines Océaniques, UMR CNRS 6538, Plouzané, France
[8] Spanish Institute of Oceanography (IEO), Oceanographic Center of Málaga, Málaga, Spain
[9] UNESCO Centre on Marine Geology and Geophysics, Moscow State University, Geology Faculty, Moscow, Russia
[10] Université Côte d'Azur, CNRS, Observatoire de la Côte d'Azur, IRD, Géoazur UMR 7329, Valbonne, France
[11] Institut de Ciències del Mar (ICM), CSIC, Continental Margins Group, Barcelona, Spain
[12] Limnological Institute, Siberian Branch of the Russian Academy of Sciences, Irkutsk, Russia

* Corresponding author : Jeffrey Poort, email address : jeffrey.poort@sorbonne-universite.fr

Abstract :

The Western Mediterranean basin has been formed by Miocene back-arc extension and is underlain by a thin and young lithosphere. This young lithosphere is warm, as testified by an overall elevated offshore heat flow. Heat flow within the Western Mediterranean is, however, highly variable and existing data are unevenly distributed and poorly studied in the central part of the Liguro-Provençal and Algero-Balearic basins. This central part is floored by a young oceanic crust, bordered by different continental margins, cut by transform faults, and filled by up to 8 km of sediments. We present a total of 148 new heat flow data collected during the MedSalt and WestMedFlux cruises in 2015 and 2016 and aligned along seven regional profiles that show an important heat flow variability on the basin-scale, but also locally on the margins.

A new heat flow map for the Western Mediterranean outlines the following regional features: (1) a higher average heat flow in the Algero-Balearic basin compared to the Liguro-Provençal basin (94 ± 13 mW/m2 and 78 ± 16 mW/m2, respectively), and (2) a regional thermal asymmetry in both basins, but with opposed heat flow trends. Up to 20% of this heat flow difference can be explained by sediment blanketing, but age and heterogeneity of ocean crust due to an asymmetric and polyphased opening of the basins are

believed to have given the major thermal imprint. Estimates of the age of the oceanic crust based on the new heat flow suggest a considerably younger West Algerian basin (16–23 Ma) compared to the East Algerian basin and the West Sardinia oceanic floor (31–37 Ma).

On the margins and ocean-continent transitions of the Western Mediterranean the new heat flow data point out the existence of two types of local anomalies (length scale 5–30 km): (1) locally increased heat flow up to 153 mW/m2 on the Gulf of Lion margin results from thermal refraction of large salt diapirs, and (2) the co-existing of both low (<50 mW/m2) and high (>110 mW/m2) heat flow areas on the South Balearic margin suggests a heat redistribution system. We suspect the lateral heat advection is resulting from a regional fluid circulation in the sediments associated to the widespread Plio-Pleistocene volcanism on the South Balearic margin.

Highlights

► 148 new heat flow data in the Western Mediterranean basin ► Significantly younger West Algerian basin compared to the East Algerian basin ► Small wavelength heat flow anomalies on the continental margins

Keywords : heat flow, Western Mediterranean Sea, Liguro-Provençal basin, Algero-Balearic basin, continental margins, oceanic crust

1. Introduction

The Liguro-Provençal and Algero-Balearic basins of the Western Mediterranean Sea are formed in a common back-arc context during the Oligocene-Miocene and floored by young oceans with similar water depth, i.e. 2800 m (Figure 1) (e.g. Rosenbaum et al., 2002; Jolivet et al., 2009; Royden and Faccenna, 2018). Their margins and ocean-continent transition (OCT) underwent, however, highly distinctive evolutions. In the Liguro-Provençal basin the Gulf of Lion margin has often been described as a non-volcanic Atlantic-type margin, whereas the volcanic west Sardinia and Corsica margins represent a continental block carrying the volcanic arc that drifted away. For the Algero-Balearic basin, transform margins have been evoked for different segments (e.g., Emile Baudot Escarpment) and its Algerian margin is nowadays in an early stage of inversion (Auzende et al., 1973; Mauffret, 2007; Roure et al., 2012). Rifting of the margins took place in a relatively short time (10 Ma at most; Séranne, 1999) along a complex subduction configuration. It has been indicated that the seafloor in the Gulf of Lion is 0.5-1 km deeper than predicted by global subsidence curves (Rehault et al., 1984; Chamot-Rooke et al., 1999; Gaillard et al., 2009; Rabineau et al., 2014), which had also been observed in the Philippine Sea back-arc basin (Lounden, 1980). The evolution of the Western Mediterranean margins can therefore have more in common with Pacific type marginal basins than classical margins (e.g. Currie and Hyndman, 2006; Kelley et al., 2006; Zhu et al., 2012).

The Western Mediterranean margins have only recently been the focus of crustal scale geophysical investigations and modelling studies (Aslanian et al., 2012; Leprêtre et al., 2013;

Medaouri et al., 2014; Mihoubi et al., 2014; Moulin et al., 2015; Afilhado et al, 2015; Bouyahiaoui et al., 2015; Aïdi et al., 2018). These studies provided some insights in nature of the ocean-continent transitions. Relying on refraction seismic data, Moulin et al. (2015) inferred that in the Gulf of Lion this transition zone is characterized by a 7 km-thick crust with « anomalous » velocities ranging from 6 to 7.5 km/s. They interpreted this as exhumed lower continental crust overlying a heterogeneous, intruded lower layer. Based on seismic reflection interpretation, Jolivet et al. (2015) suggested that the Gulf of Lion margin is underlain by a metamorphic core complex and further speculate on an exhumed mantle for the oceanic continent transition. Even if there is a large consensus that Western Mediterranean basins are floored by oceanic crust, there remains substantial speculation on the configuration, nature and evolution of its margins and the ocean-continent transitions.

Heat flow is one of the key parameters to further constrain models of crustal structure and margin evolution. The distinct overall heat flow between the Western and Eastern Mediterranean has been associated with a young, thin, hot and weak lithosphere in the west and an older, thicker, colder and stronger lithosphere in the east (inserts in Figure 1; Jiménez-Munt et al., 2003; Roure et al., 2012), but the thermal state of the margin in the Mediterranean has been poorly addressed. The thermal regime of the thinned continental margin can be modelled knowing its rifting age and the amount of crustal thinning (e.g., McKenzie, 1978) and oceanic heat flow generally follows plate cooling models (Davis and Lister, 1974; Stein and Stein, 1992; Carlson and Johnson, 1994). At the ocean-continent transition (OCT), however, lithosphere rheology is transitional and the thermo-mechanical behavior is poorly understood. The width of this OCT zone is highly variable and can attain several hundreds of km (e.g., Reston and Manatschal, 2011).

A recent detailed heat flow study of the young passive margins in the Gulf of Aden (Lucazeau et al., 2008) clearly shows contrasted thermal regimes between the oceanic/OCT and continental/proximal margin: the OCT part of the margin (distal margin) has a similar elevated heat flow as the oceanic domain which drops abruptly to background continental near the proximal margin. This suggests a persistent thermal anomaly after continental breakup (Lucazeau et al., 2008).

Other studies on other Cenozoic continental margins show that this might be a rather common and long-term feature of continental margins, e.g. Congo-Angola margin (Lucazeau et al., 2004), the Vøring basin (Scheck-Wenderoth and Maystrenko, 2008) and the Australian margins (Goutorbe et al., 2008). Lucazeau et al. (2008) suggest an ocean-continent edge-driven convection as a permanent cause for these thermal anomalies and other particular observation in margins (shallow water sediments following break-up of continents, overthickened deep margins, postrift uplifts or postrift magmatism). Several of these margin particularities have also been observed in the Western Mediterranean (e.g., Bache et al., 2010) and urge the need for a better understanding of the thermal structure of its margins.

Up to present-day, however, data in the Western Mediterranean deep basins and margins was too sparse and unevenly distributed in order to understand the thermal anomalies of higher resolution associated with OCT particular deformation, or to evaluate the effect of salt diapiric structures and volcanic seamounts on surface heat flow. Here we present a new analysis of the Western Mediterranean heat flow data in the ocean floored basins and their margins, based on a re-evaluation of existing data completed with 148 new heat flow measurements collected during the MedSalt and WestMedFlux cruises in 2015-2016. The new data were focused on the poorly studied ocean-continent transition zones and allowed us to further constrain the regional thermal imprint in the Liguro-Provençal and Algero-Balearic basins. It also showed the existence of smaller scale anomalies, both with low and high heat flow signatures. We apply a basic interpolation method to draw a strongly improved heat flow map of the Western Mediterranean that illustrates a more complex and segmented heat flow distribution that seems to have its origin in the geodynamic evolution of the back-arc opening on the one hand, and to more shallow processes occuring on the ocean-continent transition or where salt diapirism is evidenced on the other hand.

2. Geological framework

The Liguro-Provençal and Algero-Balearic basins are both considered to be formed by Oligocene-Miocene back-arc extension generated from the roll-back of the Tethys subducted oceanic crust (Rehault et al., 1984; Vigliotti and Kent, 1990; Jolivet et al., 2009). The Liguro-Provençal basin formed during a short rifting period of 9 Ma, followed by an even shorter oceanic accretion between 23-19 Ma and 16 Ma (Bache et al., 2010; Carminati et al., 2012). In the Algero-Balearic basin timing of back-arc extension is less constrained, and oceanisation has been proposed between 23 and 16 Ma (Michard et al., 2006), between 16 and 8 Ma (Mauffret et al., 2004) or from 13.8 to 11.6 Ma (Negredo et al. 1999). Seafloor-spreading history is not easily established from the available magnetic anomaly data (Galdeano and Ciminale, 1987).

For the plate kinematics during opening, there is more or less consensus for the Liguro-Provençal basin with a rotation pole located in the Gulf of Genova (Schettino and Turco, 2006; Gailler et al., 2009), while for the Algerian basin two contrasting models prevail: (1) a dominant N-S extension by a presently inactive slab under the North African Margin (Gueguen et al;, 1998; Schettino and Turco, 2006) or (2) a dominant E-W opening by a large westward rollback in the Gibraltar region (Royden, 1993; Mauffret et al., 2004). Recently, some hybrid models have been proposed (e.g. Van Hinsbergen et al., 2014; Driussi et al., 2015; Etheve et al., 2016), which equally predict large transform margins in the western part of the Algero-Balearic basin.

The Liguro-Provençal and Algero-Balearic margins also display differences in their sedimentation histories (Mauffret et al., 2004; Aslanian et al., 2012). The Pliocene and Quaternary sedimentary infill is 2 km thick in the Provençal basin but only 0.8 km thick in the Algerian basin. Moreover, the same contrast is also observed for the pre-Messinian Miocene layer, whose thickness reaches up to 4 km in the Liguro-Provençal basin but only 1.8 km thick in the Algerian basin (e.g. Rabineau et al., 2015; Arab et al., 2016). The Messinian evaporatic layer is up to 3 km thick in the Provençal basin, and about 1.2 km in the Algero-Balearic basin. This evaporitic layer is highly disturbed by diapirism in

both basins (Maillard et al., 2003; dos Reis et al., 2005; Strzerzynski et al., 2010; Acosta et al., 2013; Leprêtre et al., 2013; Dal Cin et al., 2016).

3. Review of previous heat flow data

The total amount of previous heat flow data in the Liguro-Provençal and Algero-Balearic basins consist of 365 sites, including one DSDP borehole measurement east of Minorca (site 372A: Erickson and von Herzen, 1978), one ODP south of Minorca (site 975C: Pribnow et al., 2000) and several commercial borehole estimates in the Gulf of Lion. The majority of the data are located in and near the marginal basins of Alboran, Valencia and Ligure (Della Vedova and Pellis, 1983; Foucher et al., 1992; Polyak et al., 1996; Fernandez et al., 1998; etc.). Overall heat flow data coverage is however still poor, and the uneven distribution and variable quality may easily lead to biased heat flow mapping in the Western Mediterranean.

Heat flow data acquisition in the Western Mediterranean has a long history that started in the early 1960's (figure 2), when the first marine type heat flow instruments were under development. Early devices were relatively short (2-3 m only) with only a few temperature sensors, often lacking a tilt measurement and thus vulnerable for misinterpretations. Based on a lack of basic quality control, we omitted from our heat flow data base seven pioneering data points from the 365 values available (2 from Lister, 1963; 1 from Nason & Lee, 1964, and 4 stations from the GeoMapApp database). The first eight well described measurements were made in 1965 during the Conrad cruise 9 by MIT (Erickson, 1970). The majority of the existing marine data points were obtained between 1982 and 2000, with equipment appropriate to evaluate data quality (tilt sensor, more sensors).

Some regional trends have been outlined by previous studies. In the Liguro-Provençal basin, heat flow shows a strong asymmetry from west to east, both on land and offshore (Burrus and Foucher, 1986; Lucazeau and Mailhé, 1986; Della Vedova et al;, 1995). The Hercynian basement that surrounds the basin presents a mean equilibrium heat flow of 55-65 mW/m², which appears higher in

Corsica (76 mW/m²) than in the Provence (50-60 mW/m²). Offshore, a thermal zone of very high heat flow (>100 mW/m²) exists to the east of the Provençal basin stretched all along the basin from north to south. Modelling studies have indicated that heat flow measured on the Gulf of Lion margin and further on the oceanic crust is in reasonable agreement with the expected rifting history, oceanic cooling age (Burrus and Foucher, 1986) and with first order bathymetry and gravity anomalies which contain a thermal component (Della Vedova et al., 1995). However, no model could yet predict the unusual high heat flow zone on the Sardinian margin. Various explanations have been proposed, such as a more recent opening of an ocean to the east (Rehault et al., 1984; Jemsek et al., 1985), recent intrusions of mantle material (Burrus and Foucher, 1986), renewed tectonism to the east (Della Vedova et al., 1995), asymmetric evolution during rifting (Pasquale et al., 1995), but these are generally not supported by other geological or geophysical data in the Provençal basin. For the Algero-Balearic Basin, heat flow data are even more sporadic and focused on the extreme western part (Polyak et al., 1996). Only a few values exist on the Balearic margin, with two well measurements from DSPD 371 and ODP 975. Heat flow appears elevated (80-145 mW/m²) and Mauffret et al. (2004) suggested it may correspond to an oceanic crust of 8-16 Ma.

4. Data and methods

New marine-type heat flow data were acquired during two cruises dedicated to heat flow and sediment coring in the Western Mediterranean: the MedSalt cruise on R/V OGS-Explora (OGS, Italy) in 2015 and the WestMedFlux cruise on R/V L'Atalante (Ifremer, France) in 2016. Marine heat flow, which represents the heat loss rate per unit surface area under the assumption of heat conduction, can be determined as the product of the vertical temperature gradient in the surface sediments and the thermal conductivity of the sediments.

We used two complementary instruments for heat flow acquisition: (1) a conventional multi-penetration heat flow instrument (von Herzen et al., 1989), allowing in-situ measurements of

thermal gradients and sediment thermal conductivity, was used during the WestMedFlux cruise, and (2) a sediment corer of 5 and 10 m long equipped with autonomous temperature loggers during the MedSalt and WestMedFlux cruises. Thermal conductivity of the sediment in that case was measured on-board on the recovered sediment cores. The verticality was systematically measured for both instruments, except for a few station where the tilt meter was not functioning.

4.1 Multi-penetration heat flow device

The majority of the new heat flow stations were acquired with the MCHF (Micro-Computerized Heat Flow) heat flow instrument of IPGP. It was designed by Von Herzen R.P. at Woods Hole Oceanographic Institution and upgraded significantly since 2001 at IPGP. It has a battery life of 72 hours at the bottom which allows the acquisition of multiple heat flow stations without taking the instrument back on deck (pogo type of measuring). Data acquisition is real-time controlled by an acoustic system of communication, and also recorded on a compact-flash card in the instrument.

The device has a 1.5-ton weight ensuring penetration into soft sediment of a five-meter-long barrel equipped with seven outrigger probes spaced at 59-72 cm from each other (see figure 3) that are sampled consecutively every second. The probes contain a thermistor (resolution of 0.002 K) and a heating element, allowing us to determine in-situ both sediment temperatures and the thermal conductivity. The acquisition sequence takes around 15 minutes and includes a record of the temperature decrease after a peak caused by frictional heating when the instrument penetrates into the sediment (zone 2 on figure 3), followed by the temperature increase caused by a continuous and controlled heating of the thermistors (zone 3 on figure 3). The first part of the sequence allows extrapolation of the equilibrium temperature, while the second part is used to determine in-situ thermal conductivity using the needle probe method (Von Herzen and Maxwell, 1959). With this method the temperature of the probe increases due to the controlled heating and after some time delay this increase with the logarithm of time is proportional to the inverse of thermal conductivity. The amount of successful sediment temperature and thermal conductivity measurements for each

site depends on the depth and angle of penetration, and the correct functioning of each probe. Tilt angle of the device is continuously logged.

4.2 Sediment coring heat flow determinations

The sediment coring devices of R/V OGS-Explora and R/V L'Atalante were both equipped with the same type of NKE® autonomous temperature loggers. These autonomous high-precision temperature loggers (resolution of <0.005 K) are outrigged to a sediment corer at different intervals in order to measure temperatures and thermal gradient in the sediments. An S2IP logger, added at the top of the corer, is equally autonomous and measures water depth and tilt angle of the corer. To allow frictional heat dissipation, the corer has to stay at least 7-10 minutes in sediment without tension on the cable. Logged temperature data are downloaded when the corer is back on-board. Sediment equilibrium temperatures are obtained with the same acquisition procedure as the MCHF heat flow probe.

The five meter long gravity corer used during the Medsalt cruise was equipped with 5 temperature loggers at one meter intervals. For the WestMedFlux cruise also 5 loggers were outrigged on the five meter long piston corer (0.9-1.2 m interval), while 7 temperature loggers were fixed on the ten meter long version of the corer (1.2-2.0 m interval).

Thermal Conductivity was measured on cores using the same needle-probe technique that the MCHF uses in-situ (Von Herzen and Maxwell, 1959). The needle is inserted transversally into the core in order to provide the vertical component of thermal conductivity. We used a Hukseflux device with a TP08 needle-probe and applied a heating time of 150 seconds for all measurements. We performed 3 to 8 thermal conductivity measurements on each of the 1 meter core sections.

5. Results

A total of 148 new heat flow values were obtained for the Western Mediterranean basin and margins: 113 successful measurements were obtained with the multi-penetration heat flow probe during the WestMedFlux cruise and 35 values result from coring operations equipped with loggers during the MedSalt and the WestMedFlux cruises (see figure 4 and table 1). Most of the stations have been aligned along 7 regional profiles in the Liguro-Provençal, the Algero-Balearic and the Valencia basins. A smaller number of stations were dispersed in between these regional profiles. The quality of the measurement can be evaluated from the depth of penetration, the number of sensors in the sediments and the angle of insertion, listed in the tables in the supplementary material. These tables also give coordinates of each station, water temperature, thermal gradient and average thermal conductivity.

5.1 Stations quality, thermal conductivity and thermal gradient

The majority of the new stations have a good to very good penetration (five and more of the seven sensors in the sediment) with a near-vertical insertion. Angle of penetration is on average 4.7° from the vertical for the multi-penetration probe and 1.7° for the corers. Six stations showed a large tilt between 20 and 40°, but a correction is confidently applied as a large amount of sensors penetrated into the sediments and showed net equilibrium curves. The total depth of penetration is evaluated from the individual sensor records and the angle of penetration, and averages to 4.66 m for the multi-penetration probe (for a maximum of 5.01 m) and 7 m for the corers (maximum 5-10 m depending on its configuration). The number of useful sensors for thermal gradient and thermal conductivity determination depend mainly on the length of the insertion the sediments, but was at some stations also reduced by defect sensors. An average of 93% of the mounted sensors returned in-situ determinations. The amount of thermal conductivity measurements on the cores is highly variable, and averages 21.

The measured thermal gradients for the 148 sites varied between -3 and 152 mK/m, with a mean value of 68 ±28 mK/m. Most stations showed near-linear temperature depth profiles, which is illustrated in figure 5 for the measurements along the regional profiles 1 and 3. An exception is observed at two stations, HF-09-07 and HF-09-07b, located in the Valencia through at the foot of the slope north of Minorca Island. At these two stations the temperature –depth profiles are not only non-linear, but also display a zero to negative gradient.

The thermal conductivity over the studied area varies between 0.95 and 1.67 W/m/K with a mean value of 1.14 ± 0.12 W/m/K. The in-situ measurements from the multi-penetration probe provided slightly higher values than the measurements on the recovered sediment cores (respectively, 1.16 and 1.13 W/m/K). The relative high thermal conductivity is quite normal for a land-locked basin. Thermal conductivity values show an overall increase with depth with a high scatter at all depth levels. Detrital sediment components coming from channel systems and near-surface evaporitic deposits are expected to be some of the sources of this high scatter.

5.2 New heat flow data and spatial variability

Table 1 lists two different heat flow values for each site: the heat flow measured at the surface and the heat flow obtained after a correction for sedimentation. The heat flow at the surface of the sediments is in many cases not fully representative for the heat flow at the top of the basement as it can be affected by environmental processes, such as bottom water temperature changes, heat refraction and rapid sedimentation effects. As the transient effect of the deposition of cold sediments is far the most important in most environments (Lucazeau et al., 2008), we applied a correction based on the sedimentation rate and its duration identified on the interpretation of seismic profiles (Hutchison, 1985). The sediment blanketing effect is strongest in the deep sea basins with a slightly higher effect in the Liguro-Provençal basin than in the Algero-Balearic basin (respectively 10-15% and 15-20%). On and near slope, deposits often generate a heat flow decrease

of less than 8%. Basement heat flow is thus expected to be 4 to 20% higher than the surface measured value, however, the correction is not of enough importance to significantly change local heat flow variations which remain mostly unaltered as illustrated in figure 5 for profile 1 and 3.

On the map of figure 4 we can observe that heat flow is regionally variable, with a distinct increase from north to south. The following average heat flow has been calculated for the different profiles: 62 ± 28 mW/m² for profile 1 (Golf of Lion), 73 ± 11 mW/m² for profile 2 (West Sardinia), 78 ± 11 mW/m² for profile 4 (SW Sardinia), 80 ± 23 mW/m² for profile 3 (South Baleares off Mallorca), 86 ± 32 mW/m² for profile 5 (South Baleares off Ibiza), 107 ± 9 mW/m² for profile 6 (South Baleares along slope), and 55 ± 25 mW/m² for profile 7 (NE Valencia trough).

Important local heat flow anomalies (> 110 mW/m² and < 50 mW/m²) exist along the Gulf of Lion, the south Balearic and the NE Valencia profiles. For the Golf of Lion and the South Balearic margin, both low and high heat flow anomalies seems to co-exist together, with locally values as low as 13 mW/m² and as high as 163 mW/m2. We will illustrate these observed heat flow variations along the regional heat flow profile 1 (Gulf of Lion margin) and profile 3 (South Balearic margin off Mallorca) where seismic reflection data are available to show the sedimentary settings (figure 5). Both profiles extend from the margins slope up to the deep oceanic domain over a distance of 208 km for profile 1 and 152 km for profile 2.

Along profile 1 in the Gulf of Lion (figure 5A), heat flow does not vary strongly over the whole margin and the oceanic domain. Excluding two anomalous high values, the mean heat flow remains as low as 53 ± 6 mW/m² (61 ± 7 mW/m² with sedimentation correction). Two measurement that forms an exception have values of 130 and 153 mW/m² (KF-25 and KF-26, respectively). For K26, the lateral extent of the thermal anomaly is clearly limited to 5 km, bounded by a low heat flow of 40-51 mW/m².

Along profile 3 on the South Balearic margin (figure 5B), heat flow is strongly variable for different segments of the profile. On the SE part of the profile, located in the oceanic domain of the

East Algerian basin, heat flow averages to 75 ± 6 mW/m² (84 ± 4 mW/m² with sedimentation correction). Downstream, in the OCT domain, heat flow first strongly increases up to 139 mW/m² over a short distance of 10-20 km and is then followed by a contrasting zone of low heat flow (minimum 49 mW/m²) over 15-30 km. Further landwards over the continental crust domain of the margin, heat flow increases again up to a maximum of 89 mW/m² for the most proximal part of the margin. A similar trend has been observed in the SW of the Balearic margin (see regional profile 5 on figure 4), with a very local but strong high heat of 163 mW/m² both at the foot and the top of the Emile Baudot Escarpment slope. The one at the top of the slope co-exist with a low heat flow zone of 13-53 mW/m² that stretches over maximum 15 km. The heat flow in the oceanic domain of profile 5 located in the West Algerian basin, averages to 100 ± 9 mW/m² (112 ± 10 mW/m² with sedimentation correction). This is about the 25-30 mW/m² more than in the East Algerian oceanic basin.

Smaller heat flow variations have been observed on the Sardinia margin (profiles 2 and 4) and along sections of profile 2 and 5 that cross the North Balearic fracture zone (NBFZ) that separates the the Liguro-Provençal and the Algero-Balearic basin . The Sardinia margin displays values that fluctuate between 62 and 91 mW/m², with overall the lowest values closest to the continent. For the ocean domain of the Sardinia margin, a stable heat flow of 72 ± 1 mW/m² (83 ± 1 mW/m² with sedimentation correction) is established along three stations. Heat flow over the NBFZ ranges between 44 and 87 mW/m², but without any particular trends that could distinct it from heat flow in the neighboring domains.

A distinctive low heat flow anomaly is observed in NE Valencia trough with five values ranging between -3 and 45 mW/m² (three stations are off the profile towards the Minorca slope). Two of these stations (HF-09-07 and HF-09-07b) also display atypical non-linear temperature-depth profiles (Figure 4, profile 9).

5.3 Heat flow mapping

In order to further discuss and interpret these observed heat flow trends, we present a regional heat flow contouring including the previous heat flow data set, the new stations aligned on the regional profiles and the new stations dispersed in between. This new heat flow density map of the Western Mediterranean is presented in figure 6.

For contouring the heat flow data, we adopted the natural neighbor interpolation method (Sibson, 1981; Watson, 1982). This method is designed to honor local minimum and maximum values in the point file and thereby allows the creation of accurate surface models from data sets that are very sparsely distributed or very linear in spatial distribution. It makes use of an area-weighting technique to determine a new value for every grid node with the weight based on the overlap of Voronoi polygons of the given points and the Voronoi polygon around the interpolation point. It is not a stochastic determination, but it has the advantage compared to other interpolators that the selection of neighbours is based on the configuration of the dataset, taking into account spatial variations in data density (Dumitru et al., 2013). It highlights heat flow minima and maxima represented by the input data and will not predict additional trends in data blank areas.

On the heat flow contour map we superimposed a set of regional structural elements and crustal boundaries that are important for the discussion of the heat flow. The OCT limits in the Liguro-Provençal basin are taken from Moulin et al. (2015) and Afilhado et al. (2015) and are based on refraction data interpretation from the Sardinia experiment. For the Algero-Balearic basin the ocean-continent contour is from Driussi et al. (2015) and the limit of the Hannibal structure is from Mauffret et al. (2004). The North Balearic fracture zone and other induced transform zones are based on the work of Gueguen et al. (1998), Maillard and Mauffret (1999), and Pellen et al. (2016).

6. Discussion

The 148 new heat flow measurements constitute a considerable effort to improve the heat flow coverage of the Western Mediterranean. The alignment of the data along regional profiles and the small measurements interspacing of 3-10 km allowed description of smaller scale heat flow variations than previously possible. The new heat flow density map of the Western Mediterranean (figure 6) displays both regional and local heat flow trends that can be spatially linked to different segments of the basins. We will discuss the distinct heat flow signatures for the seafloor area, the transfer zones and the continental margins, and try to relate them to tectonic, sedimentary or environmental processes that might be responsible for them (figure 7).

6.1 Western Mediterranean seafloor heat flow

The new heat flow data confirm an overall higher heat flow in the Algero-Balearic basin compared to the Liguro-Provençal basin. Based on the new grid from the heat flow contouring, heat flow averages to 78 ±16 mW/m² in the Liguro-Provençal basin and 94 ± 13 mW/m² in the Algero-Balearic basin. This heat flow trend is coherent with the progressively opening from north to south of these marine basins that started around 32-30 Ma (Rosenbaum et al., 2002; Jolivet et al., 2009). Oceanic accretion started not earlier than 23 Ma, and finished at 16 Ma in the Liguro-Provençal basin and at latest around 8 Ma in Algero-Balearic basin (Mauffret et al., 2004; Carminati et al., 2006).

In the Liguro-Provençal basin a well-defined thermal anomaly is visible in the central part of the oceanic domain. There the heat flow ranges between 70-100 mW/m², but increases to 120-140 mW/m² towards its south and north extremities. Only a few of our new stations on profile 1 and 3 fall within this oceanic domain adjacent to the OCT zone. Within the OCT zone, the new data and the map confirms the relatively low heat flow in the Gulf of Lion (50-70 mW/m²) compared to the conjugated West-Sardinia margin (70-85 mW/m²). This trend could be related to an asymmetric

evolution during rifting and ocean forming as earlier suggested (Burrus and Foucher, 1986, Pasquale et al., 1995). The recent Sardinia experiment has shown that despite a shorter transitional domain on the Sardinian side, conjugate margins show an overall symmetry with a similar intruded, heterogeneous lower continental crust (Afilhado et al., 2015). The upper crust is however distinct, with an extrusive magmatism or a very heterogeneous oceanic crust in the transition zone (Afilhado et al., 2015). A flat heat flow over the Sardinian OCT-ocean limit suggests a transition zone that is thermally more similar to the ocean domain than the continental domain.

The plate cooling model for the thermal evolution of the oceanic upper mantle has been widely accepted to explain observed variations of depth to oceanic basement and conductive heat flow with the age of seafloor younger than 80 Ma (e.g., Carlson and Johnson, 1994). Therefore, basement heat flow over the ocean domain can give us an estimation of the age of the oceanic crust formation (figure 8). For the young oceanic crust in the central part of the Liguro-Provençal basin, a basement heat flow of 139 ± 22 mW/m² suggest an age range of 9-17 Ma. This agrees well with an end of seafloor spreading at 16 Ma proposed for this basin (Bach et al., 2010). For the older oceanic domain adjacent to the Sardinia OCT, the basement heat flow is only 83 ± 1 mW/m². This implies an apparent age of 34-36 Ma, while tectonic and magmatic observations point to a considerably later start of seafloor spreading at 19-23 Ma (Carminati et al., 2012). For this age, we would expect a heat flow of 100-110 mW/m² for a normal plate cooling oceanic crust and the lower than expected heat flow suggests that the older parts of the oceanic crust have been affected by an additional cooling process.

In the Algero-Balearic basin, the regional heat flow trend is opposite to the Liguro-Provençal basin, with an overall westward increase from West-Sardinia (70-90 mW/m²) towards the Alboran basin (100 to 130 mW/m²). A north-south variation of heat flow from the South-Balearic to the Algerian margin is not well resolved because of very poor coverage over large parts of the Algerian margin and the central part of the basin. The flat contoured heat flow in north-south direction can therefore not be interpreted in relation with the direction of oceanic opening of the Algero-Balearic

basin. A good coverage of data exists on the South Balearic margin and the neighboring oceanic crust and allows to point out an important difference in thermal signature east and west of the ocean floor adjacent to the Balearic OCT. Corrected heat flow on the oceanic domain of profile 3 (off Mallorca) has a mean of 84 ± 4 mW/m², while oceanic heat flow on profile 5 (off Ibiza) reaches 112 ± 10 mW/m². It has been proposed that the Algero-Balearic basin is composed of two different oceanic basins, the West and East Algerian basin, separated by a basement structural high called the Hannibal ridge (Mauffret et al., 2004). Recent studies (Driussi et al., 2015; Aïdi et al., 2018) indicate that these two oceanic basins have different modes of opening. Taking again the heat flow-age relation of the seafloor cooling model as a reference (figure 8), we obtain a different oceanic crustal age for the West and East Algerian basin: 16-23 Ma and 31-37, respectively. For the West Algerian basin, this agrees with the period of oceanisation proposed by Michard et al. (2006) (23 and 16 Ma), while Mauffret et al., (2004) suggested a younger oceanic crust (16 and 8 Ma). They based their ages on tectonic and magmatic considerations. For the East Algerian basin, the oceanic crust near the South Balearic margin is estimated considerably older than these ages. It is remarkable that we obtain the same apparent ocean crust age on the East Algerian margin as that of the Sardinia margin. This could point to a timing and mode of opening in the East Algerian basin that is more in common with the Liguro-Provençal basin, than with the West Algerian basin. This conforms to a two-step evolution where the East Algerian opened in a NW-SE direction together with the Liguro-Provencal basin, while an east-west opening in the West Algerian only started around 16 Ma following a subcontinental-lithosphere edge delamination along the Betic-Rif margins and subsequent subduction under the Alboran basin domain (Booth-Rea et al., 2007; van Hinsbergen et al., 2014; Aïdi et al., 2018).

6.2 Transfer zones

The transition between the Liguro-Provençal and the Algero-Balearic basins is marked by the North Balearic fracture zone (NBFZ), but this zone does not display a distinctive thermal imprint. This

fracture zone has been described between the Valencia Trough and the Gulf of Lion as an important basement step of > 1km with magmatic bodies (Maillard and Mauffret, 1993; Pellen et al, 2016). For kinematic reconstruction purposes, the transform zone has been traced up to the Sicily strait (Pascuale et al., 1995), but between the Liguro-Provençal and Algero-Balearic basins it has not been evidenced by seismic data. Two of our regional heat flow profiles cross the NBFZ at two different sections, and show a heat flow that varies with a magnitude range of 40 mW/m², but without any particular trend. On the interpolated heat flow map the fracture zone seems to limit different regional heat flow domains with some of the heat flow minima and maxima located near the fracture zone. However, these heat flow anomalies are laterally still poorly constrained.

A particularly large area of low heat flow can be noticed in the north-east of the Valencia trough, between the NBFZ and the Minorca fracture zone (figure 7). As described in the results, a group of five low heat flow values with thermal gradients decreasing to zero and even negative were measured (-3 and 45 mW/m²). This confirms the small thermal gradient measurement obtained by Foucher et al. (1992) in the early 1990's at exactly the same area. They argued that it concerns a local thermal effect associated with the formation of the sedimentary ridge on which the heat flow stations are located. Indeed, a large sediment drift north of the island of Minorca resulting from the Western Mediterranean Deep Water has been described by Frigola et al. (2008). These authors point out that this bottom water current has undergone abrupt changes during the last 50 kyr, which would also imply non-stable bottom water temperature. Bottom water temperature variations will typically induce up to several meters in the sediments non-linear temperature-depth profiles and variable thermal gradients, including negative gradients (e.g. Davis et al., 2003). We therefore assume that the low heat flow zone is not a signature from deeper tectonic, sediment or hydrothermal sources, but an imprint from temperature perturbations at the sediment surface. Unfortunately, we do not have bottom water temperature time series that could allow a quantification of the expected impact on the geothermal heat flow.

6.3 Local heat flow anomalies on the margins

A particular feature outlined on the heat flow map (figures 6 and 7) is the presence of heat flow anomalies that have a limited lateral extent (5-30 km). These local anomalies of both low and high heat flow are focused on the distal continental margin and on the ocean-continent transition zone. We will distinguish two different types of local heat flow anomalies: (1) those associated with large salt domes in the Gulf of Lion margin, and (2) those on margin segments without salt diapirism.

The first type of local heat flow anomalies has been observed in the ocean-continent transition zone of the Gulf of Lion margin, where large diapiric structures characterize the Messinian unit. Two well-defined heat flow anomalies along regional profile 1 have been described in the results (maximum heat flow 130-153 mW/m²) and are also outlined on the heat flow map. Both thermal anomalies are clearly associated with the presence of a high (~3 km) and narrow (< 5 km) salt diapir directly under the measurement sites (figure 5A). One of the observed heat flow peaks is clearly limited by close-spaced data that show a normal to low heat flow at only a few kilometers distance. The observed heat flow pattern is typical for the refraction effect of a narrow salt diapir which raised up close to the sediment surface (Nagihara et al., 1992; Mello et al., 1995). Salt diapiric structures also exist in the oceanic domain of the Liguro-Provençal and Algero-Balearic basin, but we lack the heat flow data resolution in these domains to contour the thermal imprint of these higher frequency deformations.

A second type of anomalies are observed on the South Balearic margin and consists of the co-existence of local zones of both high and low heat flow as described in the results for profile 3 (off Mallorca; see figure 5) and profile 5 (off Ibiza). These anomalies are found on the distal margin, have a lateral extent of not more than 10-30 km, and reaches maxima of 140-160 mW/m² and minima of 15-50 mW/m². On the interpolated heat flow map, these anomalies are only outlined on the South Balearic margin where new detailed heat flow measurements were made. For the West Sardinia margin, we also see a local increase of heat flow on the ocean-continent transition zone close to the continent limit. Here heat flow maxima only reach values of 90-105 mW/m².

What can be the source of these local heat flow anomalies? The localization of the heat flow high on the distal margin do remind us of other margins in the world (e.g. Gulf of Aden: Lucazeau et al., 2008) where an observed thermal perturbation has been attributed to the process of edge-driven convection under a lithosphere with abrupt thickness change (King and Anderson, 1995). The width of these convection cells are estimated to be 150-500km (King and Anderson, 1998), which will produce surface heat flow anomalies that scale even larger (e.g., Hardebol et al., 2012). Edge-driven convection are thus not expected to have produced the local thermal features on the Western Mediterranean margins. A more plausible explanation are recent volcanic intrusions in the crustal and sediment column. The South Balearic margin is marked by many volcanic pinnacles composed of late Pliocene alkaline basalt (Acosta et al. 2004; Camerlenghi et al., 2009). Widespread volcanic material along the margin is also suggested by chaotic seismic reflectors and magnetic anomalies (Driussi et al., 2015). In order to create the distinct surface heat flow increase of 40-50mW/m² as observed on the South Balearic margin, a volcanic intrusion needs to be very recent (< 0.1-0.2 Ma) and at crustal depths of less than 5-10 km (e.g. Rekitake, 1995; Ritter et al., 2004). Although reported intrusions are numerous on the South Balearic and West Sardinia margin (see figure 7), none of our observed heat flow anomalies are directly located on any of the known volcanic intrusions.

Indirectly, sill intrusions could also have played a role on the thermal field by inducing hydrothermal fluid migrations. Subsea hydrothermal systems are well known at the mid-oceanic ridges (Tiveyet al., 2014) and on young sedimented ridge flanks where fluids can recharge or discharge at seamounts and flow in the uppermost basalts over distance of several tens of kilometers (e.g.; Stein and Stein, 1994, Fisher et al., 2003; Le Gal et al., 2018). But also on the continental margins and in rift basins hydrothermal systems triggered by sills have been described (Svensen et al., 2003; Berndt et al., 2016). In analogy to heat redistribution by fluid circulation near the oceanic ridges (Davis et al., 1989; Fisher et al., 2003; Wheat et al; 2004), the co-existence of low and high heat flow anomalies observed on the South Balearic margin could be sourced by a heat redistribution system. The widespread basaltic dyke and sill intrusions (Acosta et al., 2013) offer pathways for

lateral fluid migration, similar to what has been observed on the OCT of the Gulf of Aden (Lucazeau et al., 2010). Magma-driven fluid systems are not expected to be long lived and even thick intrusions can only sustain hydrothermal systems for a few thousand years (Jamtveit et al., 2004).

Other mechanisms have been proposed to explain a forced groundwater convection that affects the offshore domain. Fernandez et al. (1990) showed that a strong onshore hydraulic gradient on the NW border of the Valencia Trough permits a lateral advection of pore water about 30 km offshore along a fractured Mesozoic carbonate and could explain observed anomalous temperature gradients. Our observed local thermal anomalies on the south Balearic margin are, however, at more than 100 km distance from the shore. Another possible mechanism that may sustain a subsea groundwater circulation is dissolution of exposed Messinian evaporates. Anderson and Kirkland (1980) describe a mechanism where salt dissolution generates a brine which percolates downward through cracks and fractures as a result of its own high density and where the inflow of less salty water continues the dissolution process. This mechanism has been evoked on the Eastern Mediterranean ridge (Kastens and Spiess, 1984) and on Western Atlantic margins (Paull and Neumann, 1987), but it is still poorly documented.

Heat redistribution by a regional sub-seafloor fluid circulation system is the most plausible explanation for the observed low and high heat flow zones on the South Balearic margin, but evidence from seismic imaging and pore fluid compositions are needed to confirm that hydrothermal circulations are indeed active.

7. Conclusions

Based on a critical analysis of previously reported data and the acquisition of 148 new heat flow data in the Western Mediterranean basin, a new heat flow map is presented that displays distinct thermal features on the margins and neighboring ocean crust. A regional asymmetry of the heat flow on the oceanic crust is observed that suggests a significantly younger West Algerian basin (16-23 Ma)

compared to the East Algerian basin and West Sardinia (31-37 Ma). On different margins, the existence of small wavelength anomalies (5-30 km) of high and low heat flow has been pointed out. One type of local heat flow anomalies is associated with the heat refraction of large salt domes on the Gulf of Lion margin. The second type shows the co-existence of low and high heat flow anomalies and are found on margins where recent basaltic volcanic activity has occurred (in particular, the South Balearic margin). Here we favor the explanation of a regional heat redistribution system in the seabed: the widespread volcanic activity can bring locally heat to the surface, create favorable pathways for fluids and sustain temporarily a regional fluid circulation. These observations show that processes in the sedimentary deposits (volcanic intrusions, fluid migrations, salt deformation) can, at some stages of the margin evolution, have a more important effect on the thermicity than often assumed.

Acknowledgements

For the MedSalt cruise in 2015, we thank the captain and the crew of R/V OGS-Explora for their technical assistance. For the WestMedFlux cruise in 2016 we thank captain Gilles Ferrand and the crew of R/V L'Atalante for their professional assistance. The latter cruise and its logistic support were supported by the French naval facilities, CNRS/INSU funds through program AO/TelluS and LabexMER from the French 'Investment for the future' program.

References

Acosta, J., Ancochea, E., Canals, M., Huertas, M.J., Uchupi, E., 2004. Early Pleistocene volcanism in the Emile Baudot Seamount, Balearic Promontory (western Mediterranean Sea). Marine Geology 207, 247–257.

Acosta J., Fontán A., Muñoz A., Muñoz-Martín A., Rivera J. and Uchupi E., 2013. The morpho-tectonic setting of the Southeast margin of Iberia and the adjacent oceanic Algero-Balearic Basin. Marine and Petroleum Geology 45 (2013) 17-41.

Afilhado, A. Moulin, M., Aslanian, D., Schnürle, P., Klingelhoefer, F., Rabineau, M., Leroux, E., Beslier, M.-O., 2015. Deep Crustal Structure Across A Young Passive Margin From Wide- Angle And Reflection Seismic Data (The Sardinia Experiment) - II: Sardinia's Margin, Bulletin de la Société Géologique de France, 186 (4-5): 331-351.

Aïdi, C., Beslier, M.-O., Yelles-Chaouche, A.K., Klingelhoefer, F., Bracene, R., Galve, A., Bounif, A., Schenini, L., Hamai, L., Schnurle, P., 2018. Deep structure of the continental margin and basin off Greater Kabylia, Algeria - New insights from wide-angle seismic data modeling and multichannel seismic interpretation. Tectonophysics 728-729, 1-22.

Albert-Beltran, J.F., 1979. Heat flow and temperature gradient data from Spain. In: Cermak, V. & Rybach, L. (eds.), Terrestrial Heat Flow in Europe. Springer Verlag, Heidelberg-Berlin-New York, 261-266.

Anderson, R. and Kirkland, D., 1980. Dissolution of salt deposits by brine density flow. Geology 8 : 66--69.

Arab,M., Rabineau, M., Bracene, R., Déverchère, J., Belhai, D., Roure, F., Marok, A., Bouyahiaoui, B., Granjeon, D., Andriessen, P., Sage, F., 2016. Origin and Tectono-Sedimentary Evolution of the Eastern Algerian Basin (offshore) from Upper Oligocene to Present-Day. Marine and Petroleum Geology 77, 1355-1375.

Aslanian, D., Rabineau, M., Klingelhoefer, F., Moulin, M., Schnurle, P., Gailler, A., Bache, F., Leroux, E., Gorini, C., Droxler, A., Eguchi, N., Kuroda, J., Alain, K., Roure, F., Haq, B., 2012. Structure and evolution of the Gulf of Lions: The Sardinia seismic experiment and the GOLD (Gulf of Lions Drilling) project Leading Edge 31, 786–792.

Auzende, J.-M., Bonnin, J., Olivet, J.-L., 1973. The origin of the western Mediterranean basin. J. Geol. Soc. 129, 607–620.

Bache, F., Olivet, J.-L., Gorini, C., Aslanian, D., Labails, C. & Rabineau, M., 2010. Evolution of rifted continental margins: The case of the Gulf of Lions (Western Mediterranean Basin), Earth and Planetary Science Letters 292, 345-356.

Bassin, C., Laske, G. & Masters, G., 2000. The current limits of resolution for surface wave tomography in north america, EOS, Trans. Am. geophys. Un., 81(48), Fall Meet. Suppl., Abstract F897.

Berndt, C. , Hensen, C., Mortera-Gutierrez, C., Sarkar, S. , Geilert, S. , Schmidt, M. , Liebetrau, V., Kipfer, R., Scholz, F., Doll, M., Muff, S., Karstens, J., Planke, S., Petersen, S. , Böttner, C. , Chi, W. C., Moser, M., Behrendt, R., Fiskal, A., Lever, M. A., Su, C. C., Deng, L., Brennwald, M. S. and Lizarralde, D., 2016. Rifting under steam—How rift magmatism triggers methane venting from sedimentary basins. Geology 44 (9): 767–770.

Bookman, C.A., Malone, I. & Langseth, M.G., 1972. Sea floor geothermal measurements from conrad cruise 13, Tech. Rept. 5-CU-5-72, Columbia University, In GeoMapApp global heat-flow compilation by Abbott 2008.

Booth-Rea, G., Ranero, C., Martínez-Martínez, J.M., Grevemeyer, I., 2007. Crustal types and Tertiary tectonic evolution of the Alborán sea, western Mediterranean. G-Cubed 8, Q10004. http://dx.doi.org/10.11029/12007GC001661.

Bouyahiaoui, B., Sage, F., Abtout, A., Klingelhoefer, F., Yelles-Chaouche, K., Schnürle, P., Marok, A., Déverchère, J., Arab, M., Galve, A., Collot, J.Y., 2015. Crustal structure of the eastern Algerian continental margin and adjacent deep basin: implications for late Cenozoic geodynamic evolution of the western Mediterranean. Geophys. J. Int. 201 (3), 1912–1938.

Burrus, J., Foucher, J.P., 1986, Contribution to the thermal regime of the Provençal Basin based on flumed heat flow surveys and previous investigations: Tectonophysics 128, 303–334.

Carminati, E., M. Lustrino, and C. Doglioni (2012), Geodynamic evolution of the central and western Mediterranean: Tectonics vs. igneous petrology constraints, Tectonophysics, 579, 173–192.

Camerlenghi, A., Accettella, D., Costa, S., Lastras, G., Acosta, J., Canals, M.,Wardell, N., 2009. Morphogenesis of the SW Balearic continental slope and adjacent abyssal plain, western Mediterranean Sea. International Journal Earth Sciences 98, 735-750.

Carlson, R.L. & Johnson, H.P., 1994. On modelling the thermal evolution of the oceanic upper mantle: An asessment of the cooling plate model, J. geophys. Res., 99, 3201–3214.

Chamot-Rooke, N., Jestin, F., Gaulier, J., 1999. Constraints on Moho depth and crustal thickness in the Liguro–Provençal Basin from 3D gravity inversion: geodynamic implications. In: Durand, B., Jolivet, L., Horvath, F., Séranne, M. (Eds.), The Mediterranean Basins: Tertiary Extension within the Alpine Orogen. London Geol. Soc., Sp. Publ. 156, 37-61.

Currie, C. A., Hyndman, R. D., 2006. The thermal structure of sub-duction zone back arcs. J. Geophys. Res. 111, B08404, doi:10.1029/2005JB004024.

Dal Cin, M., Del Ben, A., Mocnik, A., Accaino, F., Geletti, R., Wardell, N., Zgur, F., Camerlenghi A., 2016. Petroleum Geoscience 22, 297-308. https://doi.org/10.1144/petgeo2015-096

Davis, E.E., Lister, C.R.B., 1974. Fundamentals of ridge crest topography. Earth Planet. Sci. Lett. 21, 405–413.

Davis, E.E., Chapman, D.S., Forster, C.B., Villinger, H., 1989. Heat-flow variations correlated with buried basement topography on the Juan de Fuca Ridge. Nature342, 533–537.

Davis, E. E., Wang, K., Becker, K., Thomson, R. E., Yashayaev, I., 2003. Deep-ocean temperature variations and implications for errors in seafloor heat flow determinations. Journal of Geophysical Research, 108(B1), 2034.

Della Vedova B., Lucazeau, F., Pasquale, V., Pellis , G., Verdoya, M., 1995. Heat flow in the tectonic provinces crossed by the southern segment of the European Geotraverse. Tectonophysics 244, 57-74.

Della Vedova, B., Pellis, G., 1983. Dati Di Flusso Di Calore Nei Mari Italiani, CNR, Roma.

Della Vedova, B., Pellis, G., 1987. Risultati delle misure di flusso di calore nel Mare di Sardegna. Gruppo Nazionale Di Geofisica Della Terra Solida, Atti Del 5° Convegno vol II, Roma, 1141-1155.

Dos Reis, A., Gorini, C. Mauffret, A., 2005. Implications of salt–sediment interactions on the architecture of the Gulf of Lions deep-water sedimentary systems—western Mediterranean Sea. Marine and Petroleum Geology 22, 713–746.

Driussi, O., Brias, A., Maillard, A., 2015. Evidence for transform motion along the South Balearic margin and implications for the kinematics of opening of the Algerian basin. Bull. Soc. géol. France, 186 (4-5): 353-370.

Dumitru P. D., Plopeanu M., Badea D., 2013. Comparative study regarding the methods of interpolation. Recent advances in geodesy and geomatics engineering. 1: 45-52.

Erickson, A.J., 1970. The Measurement and Interpretation of Heat Flow in the Mediterranean and Black Seas. PhD Thesis, Mass. Inst. Technol. and Woods Hole Ocean. Inst.

Erickson, A.J., von Herzen, R.P., 1978. Down-hole temperature measurements. Initial Report DSDP, I, 42, PT 1.

Etheve, N., Frizon de Lamotte, D., Mohna, G., Martos, R., Roca E., Blanpied, C., 2016. Extensional vs contractional Cenozoic deformation in Ibiza (Balearic Promontory, Spain): Integration in the West Mediterranean back-arc setting. Tectonophysics 682 (6), 35–55.

Fisher, A.T., Davis, E.E., Hutnak, M., Spiess, F.N., Zuhlsdorff, L., Cherkaoui, A., Christiansen, L.B., Edwards, K., Macdonald, R., Villinger, H., Mottl, M.J., Wheat, C. G., Becker, K., 2003.

Hydrothermal recharge and discharge across 50 km guided by seamounts on a young ridge flank. Nature 421, 618–621.

Fernandez, M., Marzan, I., Correia, A. and Ramalho, E., 1998. Heat flow, heat production, and lithospheric thermal regime in the Iberian Peninsula. Tectonophysics, 291(1-4): 29-53.

Fernández, M., Torné, M., Zeyen, H., 1990. Modelling of thermal anomalies in the NW border of the Valencia Trough by groundwater convection. Geophysical Research Letters, 17(1) : 105-108.

Foucher, J.P., Mauffret, A., Steckler, M., Brunet, M.F., Maillard, A., Rehault, J.P., Alonso, B., Desegaulx, P., Murillas, J., Ouillon, G., 1992. Heat flow in the Valencia trough: geodynamic implications.Tectonophysics 203,77-97. doi: 10.1016/0040-1951(92)90216-S

Frigola, J., Moreno, A., Cacho, I., Canals, M., Sierro, F. J., Flores, J. A., and Curtis, J. H., 2007. Holocene climate variability in the western Mediterranean region from a deepwater sediment record. Paleoceanography 22(2), PA2209.

Gable, R., 1979. Draft of Geothermal Flux Map of France. In: V. Cermak and L. Rybach (Editors), Terrestrial Heat Flow In Europe. Springer Verlag, Berlin, Heidelberg and New York, pp. 179-185.

Gailler, A., Klingelhoefer, F., Olivet, J.-L., Aslanian, D. and the Sardinia scientific and technical OBS teams, 2009. Crustal structure of a young margin pair: New results across the Liguro–Provençal Basin from wide-angle seismic tomography. Earth and Planetary Science Letters, 286, 333-345.

Galdeano, A., Ciminale, M., 1987. Aeromagnetic evidence for the rotation of Sardinia (Mediterranean Sea): comparison with the paleomagnetic measurements. Earth and Planetary Science Letters 82, 193-205.

Goutorbe, B., Lucazeau, F., Bonneville, A., 2008. Surface heat flow and the mantle contribution on the margins of Australia. Geochem. Geophys. Geosyst. 9, Q05011.

Goutorbe, B., Poort, J., Lucazeau, F., Raillard, S., 2011. Global heat flow trends resolved from multiple geological and geophysical proxies. Geophysical Journal International 187 (2), 1405-1419.

Gueguen, E., Doglioni, C., Fernandez, M., 1998. On the post-25 Ma geodynamic evolution of the western Mediterranean. Tectonophysics 298, 259–269.

Hutchison, I., 1985. The effects of sedimentation and compaction on oceanic heat flow. Geophysical Journal of the Royal Astronomy Society 82, 439–459.

Hutchison, I., Von Herzen, R.P., Louden, K.E., Sclater, J.G. and Jemsek, J., 1985. Heat flow in the Balearic and Tyrrhenian basins, Western Mediterranean. Journal of Geophysical Research, 90: 685-701.

Jamtveit, B., Svensen, H., Podladchikov, Y.Y., Planke, S., 2004. Hydrothermal vent complexes associated with sill intrusions in sedimentary basins. In: Breitkreuz, C., Petford, N. (Eds), Physical Geology of High-Level Magmatic Systems: Geological Society of London Special Publication 234, p. 233–241

Jemsek, J. P., Von Herzen, R. P. , Rehault, J. P. , Williams, D. L. , Sclater, J. G., 1985. Heat flow and lithospheric thinning in the Ligurian Basin (N. W. Mediterranean). Geophys. Res. Lett. 12, 693-696.

Jiménez-Munt, I., Sabadini, R., Gardi, A., Blanco, G., 2003. Active deformation in the Mediterranean from Gibraltar to Anatolia infered from numerical modelling and geodetic and seismological data. J. Geophys. Res. 108 (B1), ETG 2-1-ETG 2-24. Doi:10.1029/2001JB001544.

Jolivet, L., Faccenna, C., Piromallo, C., 2009. From mantle to crust: Stretching the Mediterranean. Earth Planet. Sci. Lett. 285, 198-209.

Jolivet, L., Gorini, C., Smit, J., Leroy, S., 2015. Continental breakup and the dynamics of rifting in back-arc basins: The Gulf of Lion margin, Tectonics 34 (4), 662-679.

Kaban, M.K., Schwintzer, P., Reigber, C., 2004. A new isostatic model of the lithosphere and gravity field, J. Geod. 78, 368–385.

Kastens, K.A., Spiess, F.N., 1984. Dissolution and collapse features on the Eastern Mediterranean Ridge. Mar. Geol. 56, 181-193.

Kelley, K.A., Plank, T., Grove, T.L., Stolper, E.M., Newman, S., Hauri, E., 2006. Mantle melting as a function of water content beneath back-arc basins. J. Geophys. Res. 111, B09.

Laske, G., Masters, G., 1997. A global digital map of sediment thickness, EOS, Trans. Am. geophys. Un., 78, F483.

Le Gal V., Lucazeau, F., Cannat, M., Poort, J., Monnin, C., Battani, A., Fontaine, F., Goutorbe, B., Rolandone, F., Poitou, C., Blanc-Valleron, M., Piedade, A., Hipolito, A., 2018. Heat flow, morphology, pore fluids and hydrothermal circulation in a typical mid-Atlantic ridge flank near Oceanographer fracture Zone, Earth and Planetary Sciences Letters. 482: 423–433.

Leprêtre, A., Klingelhoefer, F., Graindorge, D., Schnurle, P., Beslier, M.O., Yelles, K., Déverchère, J., Bracene, R., 2013. Multiphased tectonic evolution of the Central Algerian margin from combined wide-angle and reflection seismic data off Tipaza, Algeria. J. Geophys. Res.-Solid Earth 118, 1-18. http://dx.doi.org/10.1002/jgrb.50318.

Lister, C.R.B., 1963. Geothermal Gradient Measurement using a Deep Sea Corer. Geophysical Journal of the Royal Astronomical Society, 7, 571-783.

Louden, K. E., 1980. The crustal and lithospheric thicknesses of the Philippine Sea as compared to the Pacific. Earth and Planetary Science Letters 50, 275-288.

Lucazeau. F., Le Douaran, S., 1985. The blanketing effect of sediments in bastns formed by extension: a numerical model. Application to the Gulf of Ltons and Viking graben. Earth Planet. Sci. Lett. 74, 92-102.

Lucazeau, F., Mailhé, D., 1986, Heat flow, heat production and fission track data from the Hercy-nian basement around the Provençal Basin (western Mediterranean), Tectonophysics 128, 335–356.

Lucazeau, F., Brigaud, F., Bouroullec, J.L., 2004. High resolution Heat Flow Density in lower Congo basin from probe measurements, oil exploration data and BSR, Geochemistry, Geophysics, Geosystems 5, Q03001, doi:10.1029/2003GC000644.

Lucazeau, F., Leroy, S., Bonneville, A., Goutorbe, B., Rolandone, F., d'Acremont, E., Watremez, L., Düsünur, D., Tuchais, P., Huchon, P., Bellahsen, N., Al-Toubi, K., 2008. Persistent thermal activity at the Eastern Gulf of Aden after continental break-up. Nature Geoscience 1 (12), 854–858.

Lucazeau, F., Leroy, S., Rolandone, F., d'Acremont, E., Watremez, L., Bonneville, A., Goutorbe, B. & Düsünur, D. 2010. Heat-flow and hydrothermal circulations at the Ocean-Continent Transition of the Eastern Gulf of Aden. Earth Planet. Sci. Lett. 295, 554-570.

Medaouri, M., Déverchère, J., Graindorge, D., Bracene, R., Badji, R., Ouabadi, A., Yelles-Chaouche, K., Bendiab, F., 2014. The transition from Alboran to Algerian basins (Western Mediterranean Sea): chronostratigraphy, deep crustal structure and tectonic evolution at the rear of a narrow slab rollback system. J. Geod. 77, 186–205.

Maillard, A., Gaullier, V., Vendeville, B. Odonne, F., 2003. Influence of differential compaction above basement steps on salt tectonics in the Ligurian-Provençal basin, northwest Mediterranean. Marine and Petroleum Geology 20, 13–27.

Marzán, I., 2000. Régimen Térmico de la Península Ibérica. Estructura Litosférica a través del Macizo Ibério y el Margen SurPortugues. Tesis Doctoral, Universidad de Barcelona.

Mauffret, A., Frizon de Lamotte, D., Lallemant, S., Gorini, C., Maillard, A., 2004. E–W opening of the Algerian Basin (Western Mediterranean). Terra Nova 16, 257–264.

Mauffret, A., 2007. The northwestern (Maghreb) boundary of the Nubia (Africa) plate. Tectonophysics 429 (1–2), 21–44.

McKenzie, D.P., 1978. Some remarks on the development of sedimentary basins. Earth Planet. Sci. Lett. 40, 25-32.

Mello, U.T., Karner G.D., Anderson R.N., 1995. Role of salt in restraining the maturation of subsalt source rocks. Marine and Petroleum Geology 12, 697–716.

Michard, A., Negro, F., Saddiqi, O., Bouybaouene, M.L., Chalouan, A., Montigny, R., Goffé, B., 2006. Pressure–temperature–time constraints on the Maghrebide mountain building: Evidence from the Rif–Betic transect (Morocco, Spain), Algerian correlations, and geodynamic implications, C. R. Geosci. 338, 92–114.

Mihoubi, A., Schnürle, P., Benaissa, Z., Badsi, M., Bracene, R., Djelit, H., Geli, L., Sage, S., Agoudjil, A., Klingelhoefer, F., 2014. Seismic imaging of the eastern Algerian margin off Jijel: integrating wide-angle seismic modelling and multichannel seismic pre-stack depth migration. Geophys. J. Int. 198 (3), 1486-1503. doi: 10.1093/gji/ggu179.

Moulin, M., Klingelhoefer, F., Afilhado, A., Feld, A., Aslanian, D., Schnürle, P., Nouzé, H., Rabineau, M., & Beslier, M.-O., 2015. Deep crustal structure of the Gulf Of Lions margin from wide-angle and reflection seismic data (The SARDINIA experiment): Wide-Angle seismic models, Bulletin de la Société Géologique de France 186, 309-330.

Müller, R.D., Sdrolias, M., Gaina, C., Roest, W.R., 2008. Age, spreading rates, and spreading asymmetry of the world's ocean crust, Geochim. Geophys. Geosyst., 9, Q04006, doi:10.1029/2007GC001743.

Nagihara, S., Sclater, J.G., Beckley, L.M., Behrens, E.W., Lawver, L.A., 1992. High heat flow anomalies over salt structures on the Texas continental slope, Gulf of Mexico. Geophys. Res. Let. 19, 1687-1690.

Nason, P.D. , Lee, W.H.K., 1964. Heat-Flow Measurements in the North Atlantic, Caribbean and Mediterranean. Journal of Geophysical Research, 69, 4875-4883.

Negredo, A., Fernandez, M., Torne, M., Doglioni, C., 1999. Numerical modeling of simultaneousextension and compression: the Valencia Trough (western Mediterranean). Tectonics 18, 361–374.

Pasquale, V., Verdoya, M., Chiozzi, P., 1995. Rifting and thermal evolution in the Northwestern Mediterranean. Annali di Geofisica 38 (1), 43-53.

Paull, C.K., Newmann, A.C., 1987. Continental margin brine seeps: Their geological consequences. Geology, 15: 545-548.

Pellen, R., Aslanian, D., Rabineau, M., Leroux, E., Gorini, C., Silenzario, C., Blanpied, C., Rubino, J.L., 2016. The Minorca Basin: A Buffer Zone Between the Valencia and Liguro-Provençal Basins (NW Mediterranean Sea) Terra Nova 28 (4), 245-256.

Polyak, B.G., Fernandez, M., Khutorskoy, M.D., Soto, J.I., Basov, I.A., Comas, M.C., Khain, V.Y., Alonso, B., Agapova, G.V., Mazurova, I.S., Negredo, A., Tochitsky, V.O., de la Linde, J., Bogdanov, N.A., Banda, E., 1996. Heat flow in the Alboran Sea, western Mediterranean. Tectonophysics 263, 191-218.

Pribnow, D.F.C., Kinoshita, M., Stein, C.A., 2000. Thermal Data Collection and Heat Flow Recalculations for ODP Legs 101–180: Hanover, Germany (Inst. Joint Geosci. Res., Inst. Geowiss. Gemeinschaftsauf. [GGA]).

Rabineau, M., Leroux, E., Aslanian, D., Bache, F., Gorini, C., Moulin, M., Molliex, S., Droz, L., Dos Reis, T., Rubino, J-L., Olivet, J-L., 2014. Quantifying Subsidence and Isostasy using paleobathymetric markers: example from the Gulf of Lion. Earth Planet. Sci. Lett. 388, 353- 366.

Rabineau, M., Leroux, E., Aslanian, D., Bache, F., Gorini, C., Moulin, M., Molliex, S., Droz, L., Dos Reis, A.T., Rubino, J.-L., Guillocheau, F., Olivet, J.L., 2014. Quantifying subsidence and isostatic readjustment using sedimentary paleomarkers, example from the Gulf of Lion. Earth and Planet. Science Lett. 388, 1–14.

Rehault, J.P., Boillot, G., Mauffret, A., 1984, The Western Mediterranean Basin geological evolution: Marine Geology 55, 447-478.

Reston T., Manatschal G. (2011) Rifted Margins: Building Blocks of Later Collision. In: Arc-Continent Collision. Frontiers in Earth Sciences. Springer, Berlin, Heidelberg

Rosenbaum, G., Lister, G. S. and Duboz, C. 2002. Reconstruction of the tectonic evolution of the western Mediterranean since the Oligocene. In: Rosenbaum, G. and Lister, G. S. 2002. Reconstruction of the evolution of the Alpine-Himalayan Orogen. Journal of the Virtual Explorer 8, 107 - 130.

Roure, F., Casero, P., Addoum, B., 2012. Alpine inversion of the North African margin and delamination of its continental lithosphere. Tectonics 31, TC3006, doi:10.1029/2011TC002989.

Royden, L.H., 1993. Evolution of retreating subduction boundaries formed during continental collision. Tectonics 12 (3), 629-638.

Royden, L., Faccenna, C., 2018. Subduction Orogeny and the Late Cenozoic Evolution of the Mediterranean Arcs. Annu. Rev. Earth Planet. Sci. 46: 261–89.

Scheck-Wenderoth, M., Maystrenko, Y., 2008. How warm are passive continental margins? A 3-D lithosphere-scale study from the Norwegian margin. Geology 36, 419–422.

Séranne, M., 1999. The gulf of Lion continental margin (NW Mediterranean) revisited by IBS: an overview. In Durand, B., Jolivet, L., Horvath, F & Séranne M., (Eds), The Mediterranean Basins: Tertiary Extension Within the Alpine Orogen. Geol. Soc. of London, Special Publication 156, 15-36.

Schettino, A., Turco, E., 2006. Plate kinematics of the western Mediterranean region during the Oligocene and early Miocene, Geophys. J. Int., 166 1398–1423.

Sengör, A.M.C., Natal'in, B.A., 2001. Rifts of the world, in Mantle Plumes: Their Identification Through Time, pp. 389–482, eds Ernst, R.E.& Buchan, K.L., Geological Society of America Special Paper 352.

Shapiro, N.M., Ritzwoller, M.H., 2004. Inferring surface heat flux distributions guided by a global seismic model: particular application toAntarctica, Earth planet. Sci. Lett. 223, 213–224.

Siebert, L.&Simkin, T., 2002. Volcanoes of the world: an illustrated catalog of holocene volcanoes and their eruptions, Tech. Rep. GVP-3, Smithsonian Institution, Global Volcanism Program Digital Information Series, http://www.volcano.si.edu/world/, last accessed January 18, 2009.

Sibson, R., 1981. A Brief Description of Natural Neighbor Interpolation, Chapter 2 in Interpolating multivariate data, John Wiley & Sons, New York, 1981, pp. 21-36.

Subono, S., 1983. Flux de Chaleur Terrestre dans la région Sud Est de la France. DEA Thesis, USTL, Montpellier.

Stein, C.S., Stein, S., 1992. A model for the global variation in oceanic depth and heat flow with lithospheric age. Nature359, 123–129.

Stein, C. S., Stein, S., 1994. Constraints on hydrothermal heat flux through the oceanic lithosphere from global heat-flow, Journal of Geophysical Research 99 (B2), 3081-3096.

Stein, C.A., and Von Herzen, R.P., 2007, Potential effects of hydrothermal circulation and magmatism on heatflow at hotspot swells, in Foulger, G.R., and Jurdy, D.M., eds., Plates, plumes, and planetary processes: Geological Society of America Special Paper 430, 261–274, doi: 10.1130/ 2007.2430(13).

Strzerzynski, P., Déverchère, J., Cattaneo, A., Domzig, A., Yelles, K., de Lepinay, B.M., Babonneau, N., Boudiaf A., 2010. Tectonic inheritance and Pliocene-Pleistocene inversion of the Algerian margin around Algiers: Insights from multibeam and seismic reflection data, Tectonics, 29, TC2008.

Svensen, H., Planke, S., Jamtveit, B., and Pedersen, T., 2003. Seep carbonate formation controlled by hydrothermal vent complexes: A case study from the Vøring Basin, the Norwegian Sea. Geo-Marine Letters, 23: 351–358.

Tivey, M., 2014. Black and White Smokers. In: Harff J., Meschede M., Petersen S., Thiede J. (eds) Encyclopedia of Marine Geosciences. Springer, Dordrecht

Van Hinsbergen, D. J. J., Vissers, R. L. M. , Spakman, W., 2014. Origin and consequences of western Mediterranean subduction, rollback, and slab segmentation. Tectonics 33, 393-419.

Vigliotti, L., Kent, D.V., 1990. Paleomagnetic results of Tertiary sediments from Corsica: evidence of post-Eocene rotation. Physics of the Earth and Planetary Interiors 62, 97-108.

Von Herzen, R.P., Hutchison, I., Jemsek, J. and Sclater, J.G., 1982. Geothermal Flux In Western Mediterranean Basins. EOS Trans. AGU.

Watson, D., 1992. Contouring: A Guide to the Analysis and Display of Spatial Data,Pergamon Press, London.

Wheat, C.G., Mottl, M.J., Fisher, A.T., Kadko, D., Davis, E.E., Baker, E.T., 2004. Heat flow through a basaltic outcrop on a sedimented young ridge flank. Geochem. Geophys. Geosyst.5 (12), Q12006.

Zhu, J., Qiu, X., Kopp, H., Xu, H., Sun, Z., Ruan, A., Sun, J., Wei, X., 2012. Shallow anatomy of a continent–ocean transition zone in the northern South China Sea from multichannel seismic data. Tectonophysics 554–557: 18–29

Zolotarev and A.V. Kondurin and V.V. Sochelnikov, 1989. Internal Report, Institute Okeanologia, Moskva.

Figure captions

Figure 1. Regional tectonic setting of the Mediterranean basin, illustrating the young oceanic crust in the Western Mediterranean formed by back-arc extension (from Jolivet et al., 2009). The white inset frame is the study area. The inset maps below show the heat flow and the lithospheric thickness of the Mediterranean basins (from Jiménez-Munt et al., 2003): a hot Western Mediterranean with a thin lithosphere contrasts with a cold Eastern Mediterranean. Modified after Roure et al. (2012).

Figure 2. The distribution of existing offshore heat flow data illustrating the poor coverage. Color coding shows the year of data collection, which were mostly in the 1970's. Circles are marine-type heat flow measurements and triangles are heat flow estimates from offshore drill holes. Reference code numbers: (1) Lister, 1963; (2) Nason and Lee, 1964; (3) Erickson, 1970; (4) GeoMapApp database; (5) Von Herzen et al., 1982; (6) Della Vedova and Pellis, 1983; (7) Jemsek et al., 1985; (8) Hutchison et al., 1985); (9) Burrus and Foucher, 1986; (10) Della Vedova and Pellis, 1983; (11) Zolotarev et al., 1989; (12) Foucher et al., 1992; (13) Polyak et al., 1996; (14) Fernandez et al., 1998; (15) Marzan, 2000; (16) Erickson and von Herzen, 1978; (17) Albert-Beltran, 1979; (18) Gable, 1979; (19) Subono, 1983; and (20) Pribnow et al., 2000.

Figure 3. Illustration of the multi-penetration heat flow probe indicating the main measuring elements (left panel) and the heat flow measurement sequence for this device (right panel). The sequence shows a two-step acquisition of in-situ temperature (zone 2) and thermal conductivities (zone 3). The heat flow coring device follows the same principle, but thermal conductivities are not measured in-situ but on-board on the cores. The equilibrium sediment temperatures, thermal gradients, thermal conductivities and heat flow are processed later on-board

Figure 4. The 148 new heat flow values obtained in the Western Mediterranean during the MedSalt-2015 and WestMedflux-2016 cruises (squares and triangles are data acquired respectively with

the multi-penetration probe and the heat flow coring device).The majority of the data are located along 7 regional profiles that cross the ocean-continent transitions (ocean floor part of the deep basins are indicated by blue) and the North Balearic fracture zone (NBFZ). Previous data that were validated by a quality check, are also plotted for comparison (small dots).

Figure 5. The heat flow variability and the temperature-depth data along two selected regional profiles: (A) profile 1 in the Gulf of Lion margin and (B) profile 3 in the South Balearic margin. These examples illustrate the presence of two types of local heat flow anomalies on the margins: those associated with large salt domes in the Gulf of Lion margin, and those where both low and high heat flow zones of 10-30 km in width co-exist on the South-Balearic margin. Limits for the oceanic and continental crust and the transition zone in between (OCT) are drawn based on work of Moulin et al. (2015) and Driussi et al. (2015).

Figure 6. New heat flow contour map of the Western Mediterranean based on an interpolation with the natural neighbor method using the cleaned existing data base and the newly acquired data. The map shows a regional heat flow asymmetry in both the Liguro-Provençal and Algero-Balearic basins with opposite directions, and the emergence of small wavelength anomalies of high and low heat flow on the continental margins.

Figure 7. A highlight of the regional heat flow trends and the different local heat flow anomalies of the Western Mediterranean discussed in the text. We also plotted the distribution of volcanic intrusion that are evoked in the interpretations and the Hannibal ridge that divides the East and West Algerian basins. Squares with numbers 1 to 4 corresponds to the seafloor areas used to estimate an age of the oceanic crust (see figure 8).

Figure 8. A relation between the basement heat flow and the age of the oceanic seafloor can be considered in case a plate cooling model is valid in the region (Carlson and Johnson, 1994). For four selected regions of the oceanic part of the Western Mediterranean we plotted the mean heat flow and its standard variation on this graphic (see figure 7 for location of the regions). The

resulting “apparent” ages are discussed in the text and compared with age estimates from geodynamic studies.

HF site name	Profile or zone	WD (m)	HFmes	HFcor	σHF
			(mW/m²)		
HF-01-01	GoL	2459	54.5	65.2	6.3
HF-01-02	GoL	2432	60.8	72.2	7.1
HF-01-03	GoL	2400	57.4	69.0	4.9
HF-01-04	GoL	2364	60.4	71.9	4.4
HF-02-01	Profile 1	2631	61.5	72.6	6.4
HF-03-01	Profile 3	2833	71.4	81.3	5.8
HF-03-02	Profile 3	2812	71.9	81.8	3.9
HF-03-03	Profile 3	2783	81.3	88.2	6.9
HF-03-04	Profile 3	2717	139.4	151.2	11.9
HF-03-05	Profile 3	2716	105.4	114.8	5.0
HF-03-06	Profile 3	2676	107.4	114.4	21.9
HF-03-07	Profile 3	1960	74.8	79.0	3.6
HF-03-08	Bal	1964	67.4	74.0	2.0
HF-03-09	Bal	2100	86.9	91.9	1.8
HF-03-10	Bal	2307	86.7	91.9	3.1
HF-03-12	Bal	2406	106.4	117.6	7.4
HF-04-01	Profile 3	2126	78.4	82.6	3.9
HF-04-02	Profile 3	2301	56.5	58.5	2.3
HF-04-03	Profile 3	2552	49.2	53.4	1.5
HF-04-04	Profile 3	2541	69.1	76.5	2.4
HF-04-05	Profile 3	2616	68.7	75.6	3.1
HF-05-01	Profile 4	2859	95.3	108.0	6.8
HF-05-02	Profile 4	2859	71.8	81.3	5.1
HF-05-03	Profile 4	2859	94.3	104.6	6.9
HF-05-04	Profile 4	2858	86.6	96.7	7.1
HF-05-05	Profile 4	2858	72.5	82.0	8.4
HF-05-06	Profile 4	2855	69.7	78.7	2.9
HF-05-07	Profile 4	2853	88.4	101.3	4.9
HF-05-08	Profile 4	2542	76.5	78.8	2.5
HF-05-09	Profile 4	2212	71.1	77.2	6.2
HF-05-10	Profile 4	1968	66.5	72.0	1.2
HF-06-01	Profile 2	2067	84.7	89.4	1.6
HF-06-02	Profile 2	2238	59.1	64.8	2.7
HF-06-03	Profile 2	2578	91.2	102.5	4.3
HF-06-06	Profile 2	2854	72.4	83.8	5.4
HF-06-07	Profile 2	2857	71.9	83.3	6.1
HF-06-08	Profile 2	2855	71.5	81.3	6.6
HF-06-09	Profile 2	2856	71.9	83.0	6.5
HF-07-01	Profile 5	1231	57.6	59.8	3.6
HF-07-02	Profile 5	1408	13.1	13.8	1.5
HF-07-03	Profile 5	1614	38.6	40.2	1.8
HF-07-04	Profile 5	1834	50.2	53.3	1.7
HF-07-05	Profile 5	2034	83.9	88.4	4.9
HF-07-06	Profile 5	2590	100.9	104.8	2.4
HF-07-07	Profile 5	2625	87.0	90.6	1.7
HF-07-08	Profile 5	2644	89.4	95.1	4.1
HF-07-09	Profile 5	2656	91.1	98.1	4.7
HF-07-10	Profile 5	2684	100.2	107.3	3.8
HF-07-11	Profile 5	2704	93.8	99.9	5.9
HF-07-12	Profile 5	2796	85.4	89.8	4.7
HF-07-14	Profile 5	2810	126.8	134.8	5.4
HF-07-15	Profile 5	2809	103.6	112.3	3.5
HF-07-16	Profile 5	2807	86.8	94.9	9.2
HF-07-17	Profile 5	2807	62.9	70.2	3.3
HF-07-18	Profile 5	2807	78.5	86.8	4.6
HF-07-19	Profile 5	2812	89.7	99.6	6.6
HF-07-20	Profile 5	2806	97.5	108.6	4.6
HF-07-21	Profile 5	2809	91.3	103.8	7.4
HF-07-22	Profile 5	2806	116.8	131.2	11.8
HF-07-23	Profile 5	2808	105.7	118.9	7.6
HF-07-24	Profile 5	2807	99.7	112.6	15.9
HF-07-25	Profile 5	2804	95.0	107.2	7.4
HF-07-26	Profile 5	2806	91.2	102.1	5.7
HF-08-01	Profile 6	2770	103.8	113.7	3.6
HF-08-02	Profile 6	2769	104.0	114.1	1.9
HF-08-03	Profile 6	2777	127.4	138.4	2.6
HF-08-04	Profile 6	2784	105.5	109.7	5.1
HF-08-05	Profile 6	2780	114.3	119.1	5.1
HF-08-06	Profile 6	2734	111.5	116.1	6.1
HF-08-07	Profile 6	2738	98.2	104.2	4.1
HF-08-08	Profile 6	2727	103.1	111.0	2.7
HF-08-09	Profile 6	2692	106.6	114.1	8.5
HF-08-10	Profile 6	2585	116.0	121.9	8.9
HF-08-11	Profile 6	2509	100.6	107.9	3.6

HF site name	Profile or zone	WD (m)	HFmes	HFcor	σHF
			(mW/m²)		
HF-08-12	Profile 6	2489	94.6	101.2	3.3
HF-08-13	Bal	2801	159.6	163.1	5.0
HF-08-14	Bal	2732	136.2	145.1	4.6
HF-08-15	Bal	1465	6.8	7.1	1.2
HF-08-16	Profile 5	1485	32.5	34.7	2.2
HF-08-17	Bal	1465	163.2	171.5	4.5
HF-08-18	Profile 5	1330	52.7	55.4	2.0
HF-09-01	Profile 7	1792	98.8	103.5	5.0
HF-09-02	Profile 7	1967	61.3	64.3	2.2
HF-09-04	Profile 7	2147	15.6	16.7	3.4
HF-09-05	Profile 7	2242	43.0	45.6	2.5
HF-09-06	Val	2233	17.2	19.0	2.0
HF-09-07	Val	2183	0.7	0.8	6.4
HF-09-07b	Val	2185	-3.1	-3.4	7.9
HF-09-08	Profile 7	2471	67.9	75.1	3.4
HF-09-09	Profile 7	2503	62.6	70.4	2.3
HF-09-10	Profile 7	2516	79.2	88.8	5.2
HF-09-11	Profile 7	2492	43.7	48.5	3.7
HF-09-12	Profile 7	2541	61.1	66.8	3.8
HF-09-13	Profile 7	2541	43.1	47.8	2.2
HF-09-14	GoL	2613	80.3	92.9	21.7
HF-10-01	Profile 1	1494	51.5	56.1	3.2
HF-10-02	Profile 1	1717	62.4	68.3	1.7
HF-10-03	Profile 1	1805	51.7	57.6	2.0
HF-10-04	Profile 1	1924	54.5	61.5	2.3
HF-10-05	Profile 1	1989	54.2	60.9	2.0
HF-10-06	Profile 1	2117	48.6	55.5	1.5
HF-10-07	GoL	2206	60.3	69.3	3.2
HF-10-08	Profile 1	2309	50.4	57.8	2.7
HF-10-09	Profile 1	2372	59.9	68.9	2.1
HF-10-10	Profile 1	2387	57.1	66.9	2.6
HF-10-11	Profile 1	2403	62.7	74.1	2.7
HF-10-12	Gol	2514	60.6	70.5	2.3
HF-10-13	Gol	2479	54.1	63.5	2.9
HF-10-14	Gol	2477	55.9	65.5	2.2
HF-10-15	Profile 1	2507	55.8	64.6	2.4
HF-10-17	Gol	2497	53.8	62.4	2.2
HF-10-18	Gol	2455	40.1	47.4	1.2
HF-10-19	Gol	2422	45.4	53.3	1.9
GC-01	Bal	2795	110.7	125.5	6.5
GC-02	Bal	2791	86.0	95.9	5.0
GC-03	Profile 5	2643	85.3	93.2	4.2
GC-06	Bal	1401	29.6	32.1	2.3
GC-07	Bal	791	91.1	94.6	6.3
GC-09	Bal	1012	60.6	63.9	5.3
GC-10	Bal	1026	72.3	79.1	15.8
GC-11	Bal	807	67.3	71.7	9.7
KF-01	GoL	2331	58.3	70.2	5.5
KF-03	Bal	2173	94.3	98.9	7.6
KF-04	Profile 3	2858	68.3	77.0	9.1
KF-05	Profile 2	2017	61.9	68.3	11.0
KF-06	Bal	2149	105.3	110.9	9.7
KF-07	Profile 3	1671	89.4	93.2	8.7
KF-08	Bal	2720	92.7	101.6	6.8
KF-09	Bal	2730	100.8	110.7	18.0
KF-10	Profile 5	2805	95.4	106.3	7.7
KF-11	Profile 5	2803	88.3	99.6	12.0
KF-12	Bal	2800	83.3	110.0	5.1
KF-13	Bal	2714	82.0	91.4	4.4
KF-14	Bal	2766	130.3	145.3	8.1
KF-15	Bal	2747	123.9	140.9	11.0
KF-16	Bal	1429	21.3	22.4	2.1
KF-17	Bal	1470	146.7	154.2	12.0
KF-18	Bal	2803	163.1	171.3	21.0
GF-19	Bal	2651	79.9	89.9	11.0
KF-20	Val	2152	2.3	2.5	1.0
KF-21	GoL	2535	57.3	67.2	3.8
KF-22	Profile 1	2425	52.5	61.6	5.6
KF-23	Profile 1	1268	44.6	50.2	5.7
KF-24	GoL	2266	52.9	62.8	5.3
KF-25	Profile 1	2283	153.4	185.9	12.0
KF-26	Profile 1	2471	129.6	150.2	7.0
KF-27	Profile 1	2540	50.0	58.3	5.0
KF-28	Profile 1	2602	53.7	62.9	6.0

Table 1. Results of the 148 heat flow sites acquired with the multi-penetration MCHF device (prefix HF) and with sediment cores equipped with temperature loggers (prefix GC for the MedSalt cruise and KF & GF for the WestMedFlux). “HFmes” is the measured heat flow based on a tilt-corrected thermal gradient and thermal conductivity determinations (see table in annex for details), “HFcor” is the heat flow corrected for the sedimentation effect, and “σHF” is the standard error on corrected heat flow values. WD is the water depth measured by the multibeam. Majority of sites are located on regional profiles (see figure 4); sites off-profile are located in the following zones: “GoL” is Gulf of Lion, “Bal” the Balearic promontory and South Balearic margin, and “Val” the Valencia through. Exact location of each site can be found in the table in annex.

Declaration of interests

☒ The authors declare that they have no known competing financial interests or personal relationships that could have appeared to influence the work reported in this paper.

☐The authors declare the following financial interests/personal relationships which may be considered as potential competing interests:

Highlights

- 148 new heat flow data in the Western Mediterranean basin
- Significantly younger West Algerian basin compared to the East Algerian basin
- Small wavelength heat flow anomalies on the continental margins

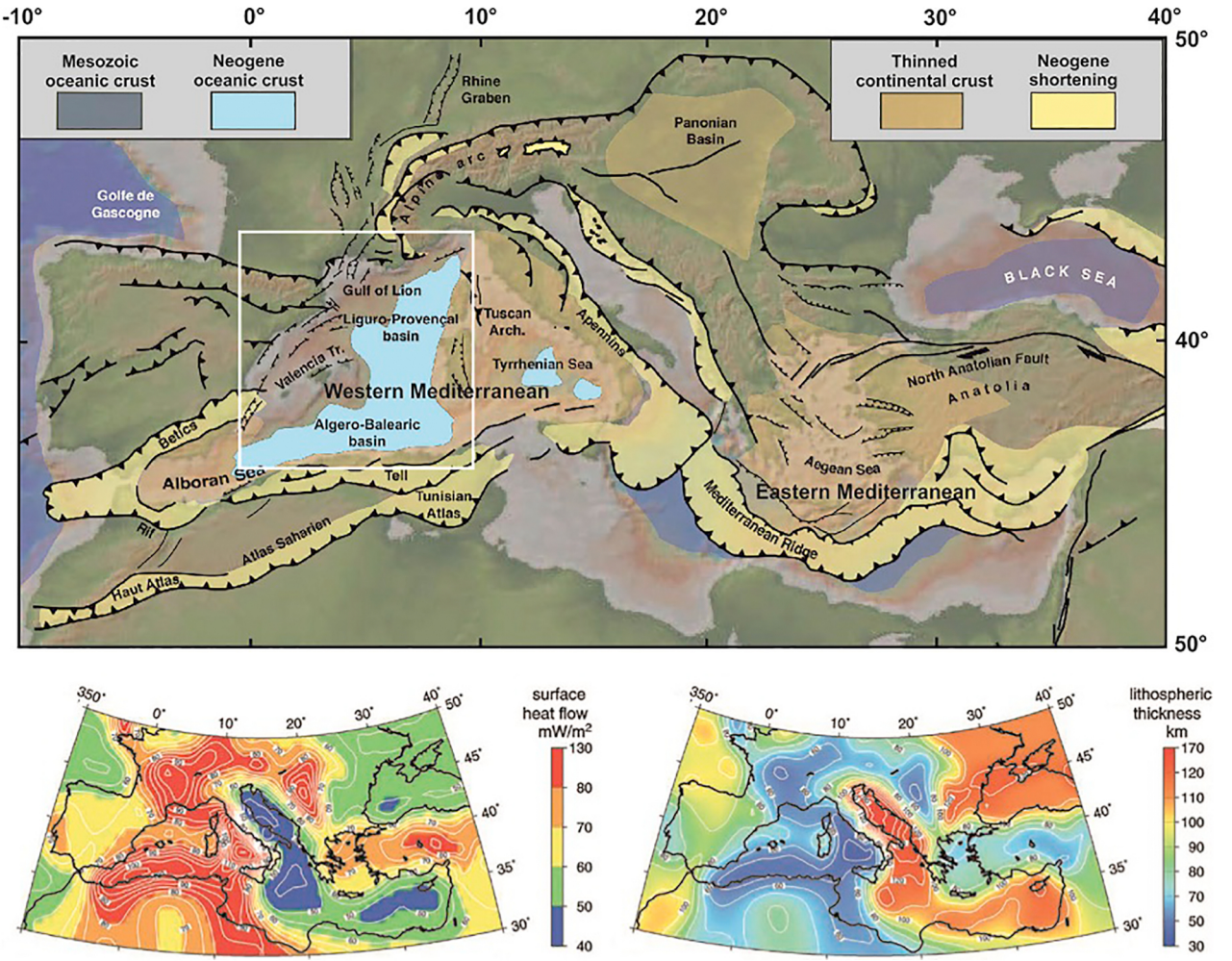
-10°
0°
10°
20°
30°
40°
50°
40°
50°
Mesozoic oceanic crust
Neogene oceanic crust
Thinned continental crust
Neogene shortening
Rhine Graben
Panonian Basin
Alpine arc
Golfe de Gascogne
Gulf of Lion
Liguro-Provençal basin
Tuscan Arch.
Apennins
Valencia Tr.
Tyrrhenian Sea
Western Mediterranean
Algero-Balearic basin
Betics
Alboran Sea
Tell
Tunisian Atlas
Rif
Atlas Saharien
Haut Atlas
BLACK SEA
North Anatolian Fault
Anatolia
Aegean Sea
Eastern Mediterranean
Mediterranean Ridge
surface heat flow mW/m²
130
80
70
60
50
40
lithospheric thickness km
170
120
110
100
90
80
70
50
30

Figure 1

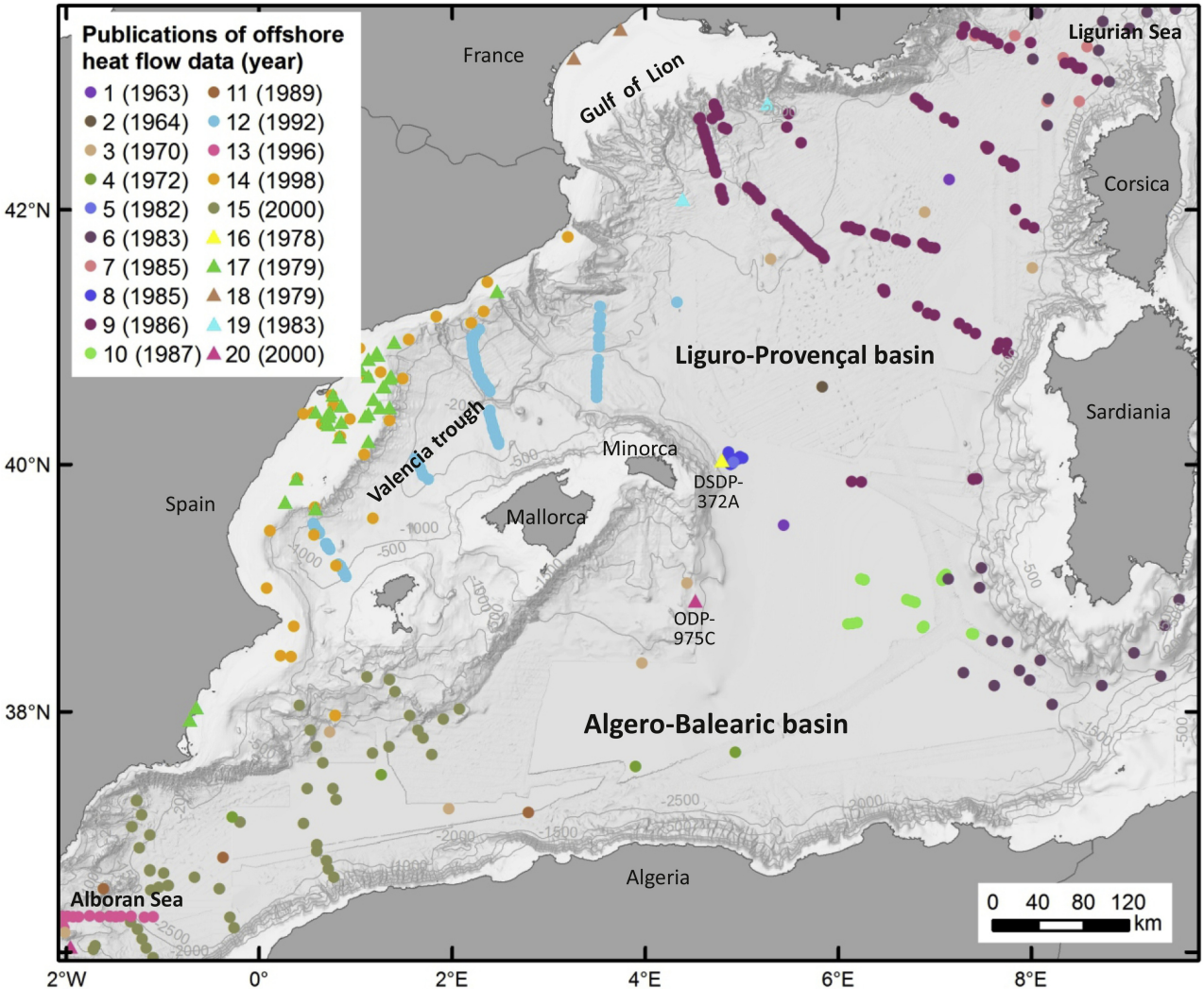
Publications of offshore heat flow data (year)
1 (1963)
2 (1964)
3 (1970)
4 (1972)
5 (1982)
6 (1983)
7 (1985)
8 (1985)
9 (1986)
10 (1987)
11 (1989)
12 (1992)
13 (1996)
14 (1998)
15 (2000)
16 (1978)
17 (1979)
18 (1979)
19 (1983)
20 (2000)
France
Gulf of Lion
Ligurian Sea
Corsica
Sardiania
Liguro-Provençal basin
Valencia trough
Minorca
Mallorca
DSDP-372A
ODP-975C
Spain
Algero-Balearic basin
Algeria
Alboran Sea
0 40 80 120 km
42°N
40°N
38°N
2°W
0°
2°E
4°E
6°E
8°E

Figure 2

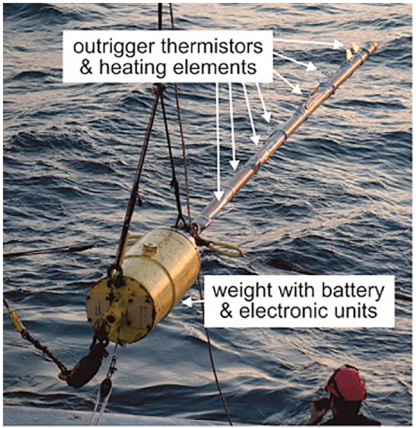
outrigger thermistors
& heating elements
weight with battery
& electronic units

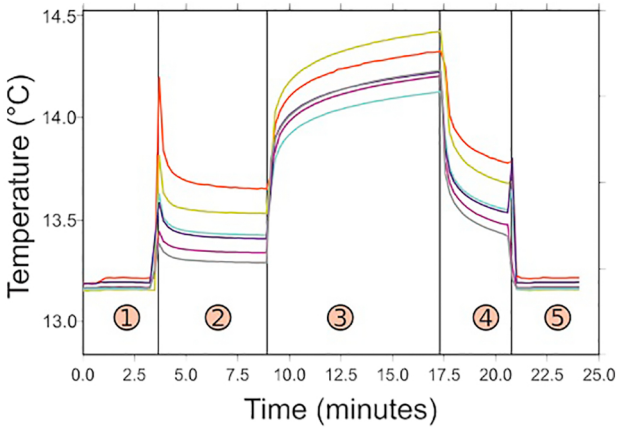
Temperature (°C)
14.5
14.0
13.5
13.0
①
②
③
④
⑤
0.0
2.5
5.0
7.5
10.0
12.5
15.0
17.5
20.0
22.5
25.0
Time (minutes)

Figure 3

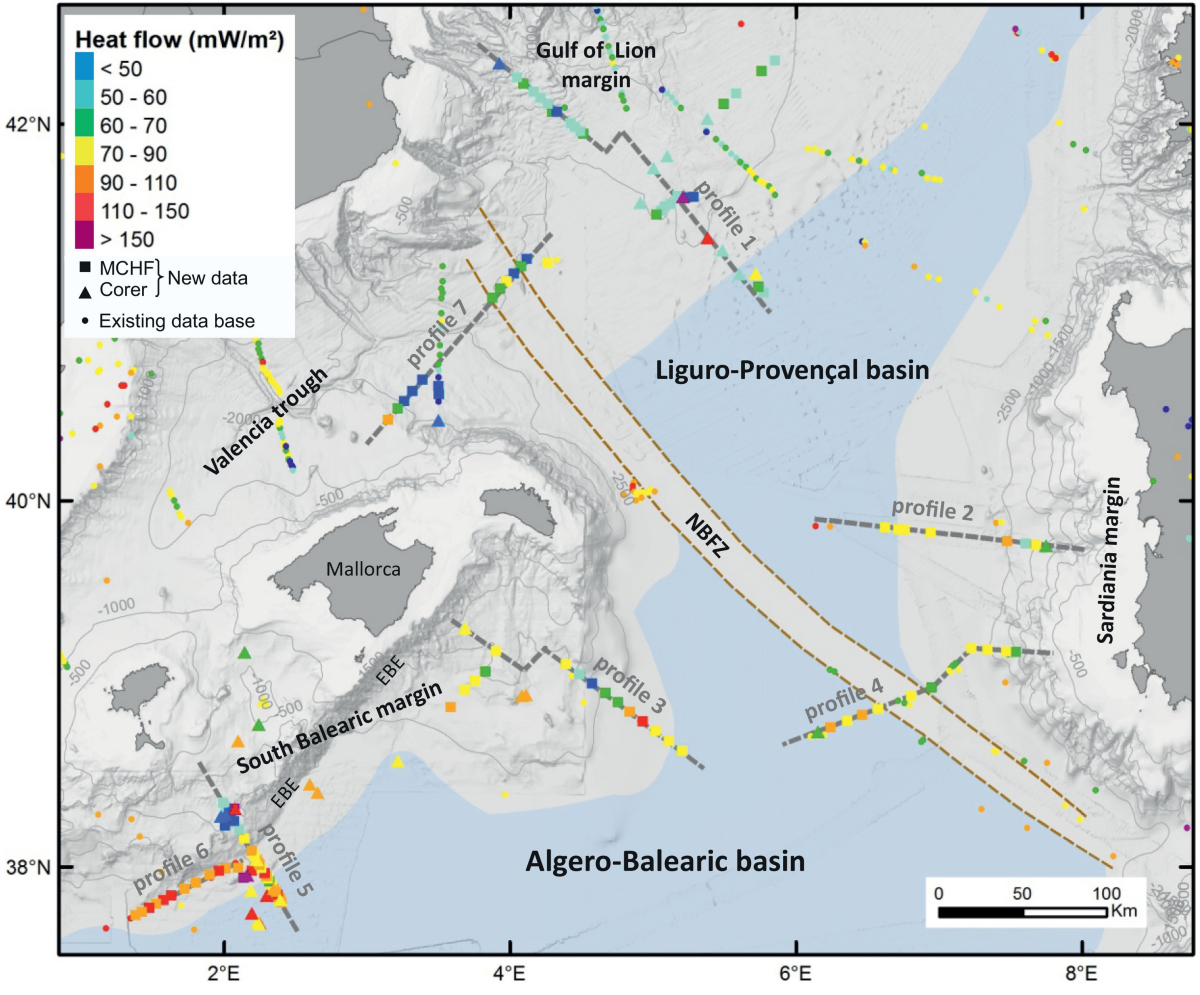
Heat flow (mW/m²)
< 50
50 - 60
60 - 70
70 - 90
90 - 110
110 - 150
> 150
MCHF
Corer
New data
Existing data base
Gulf of Lion margin
profile 1
profile 7
Valencia trough
Liguro-Provençal basin
NBFZ
profile 2
Sardiania margin
Mallorca
EBE
South Balearic margin
profile 3
profile 4
EBE
profile 6
profile 5
Algero-Balearic basin
0
50
100
Km
42°N
40°N
38°N
2°E
4°E
6°E
8°E

Figure 4

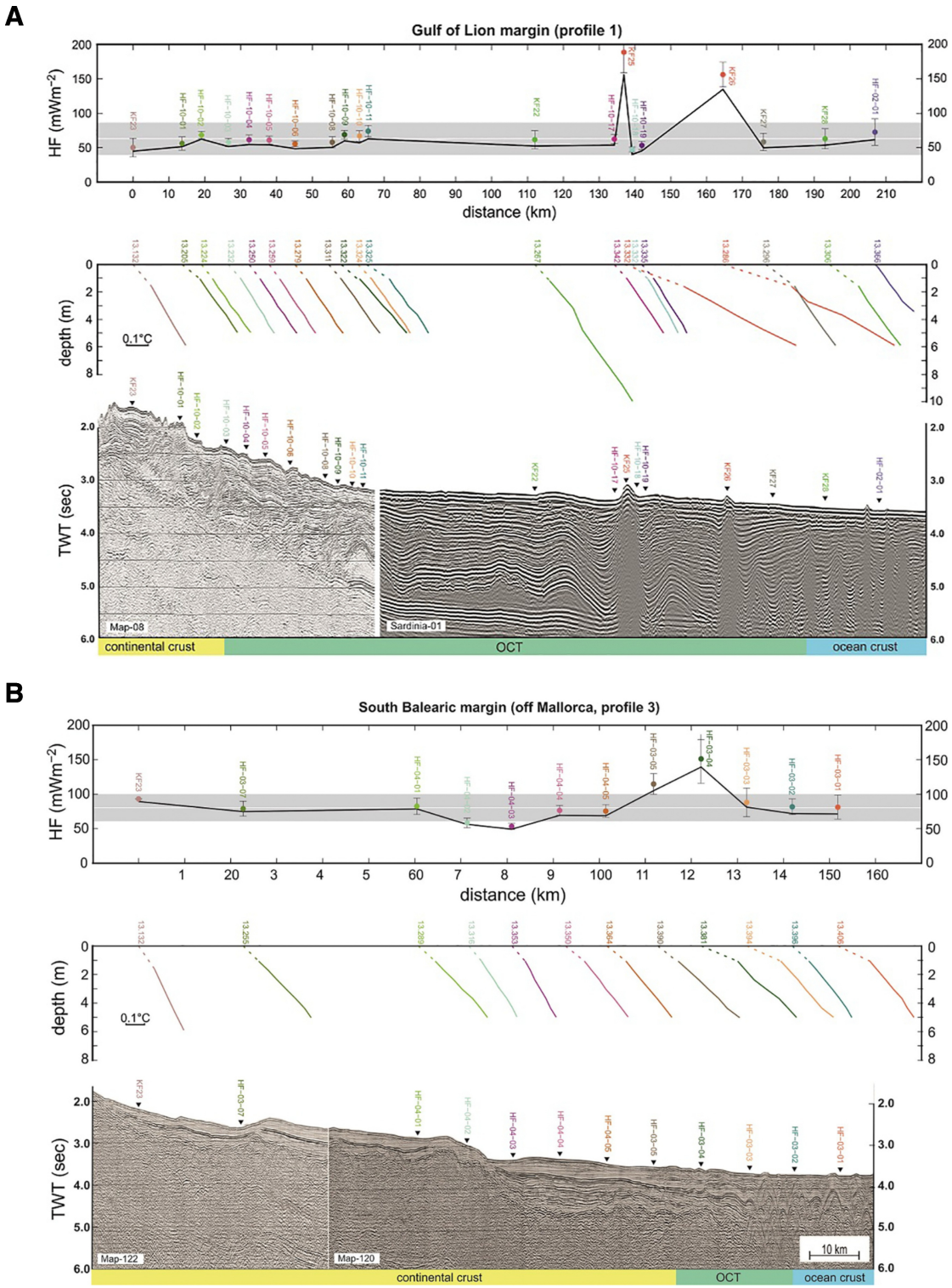
A
Gulf of Lion margin (profile 1)
HF (mWm-2)
distance (km)
depth (m)
0.1°C
TWT (sec)
Map-08
Sardinia-01
continental crust
OCT
ocean crust
B
South Balearic margin (off Mallorca, profile 3)
HF (mWm-2)
distance (km)
depth (m)
0.1°C
TWT (sec)
Map-122
Map-120
10 km
continental crust
OCT
ocean crust

Figure 5

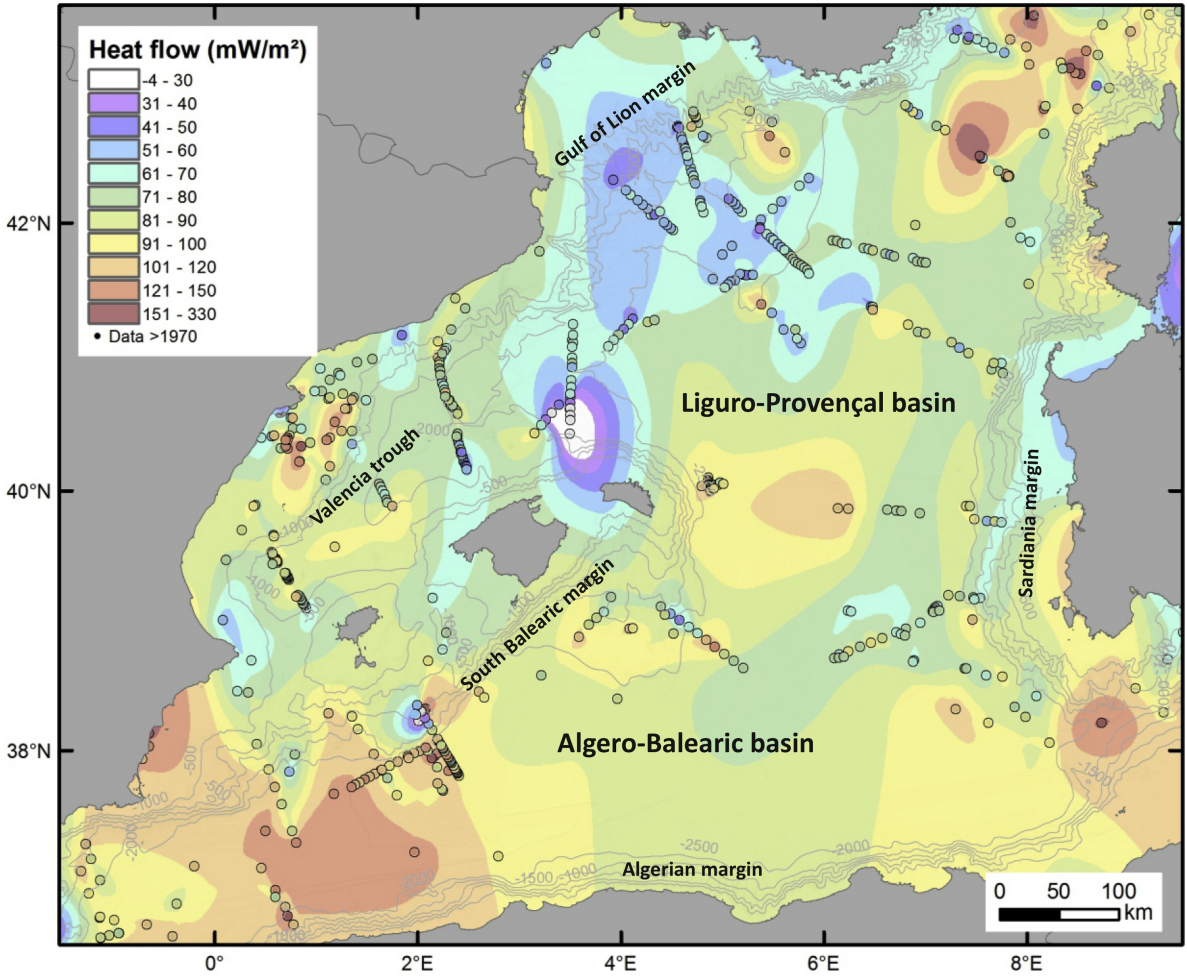
Heat flow (mW/m²)
-4 - 30
31 - 40
41 - 50
51 - 60
61 - 70
71 - 80
81 - 90
91 - 100
101 - 120
121 - 150
151 - 330
• Data >1970
Gulf of Lion margin
Liguro-Provençal basin
Valencia trough
South Balearic margin
Sardiania margin
Algero-Balearic basin
Algerian margin
42°N
40°N
38°N
0°
2°E
4°E
6°E
8°E
0 50 100
km

Figure 6

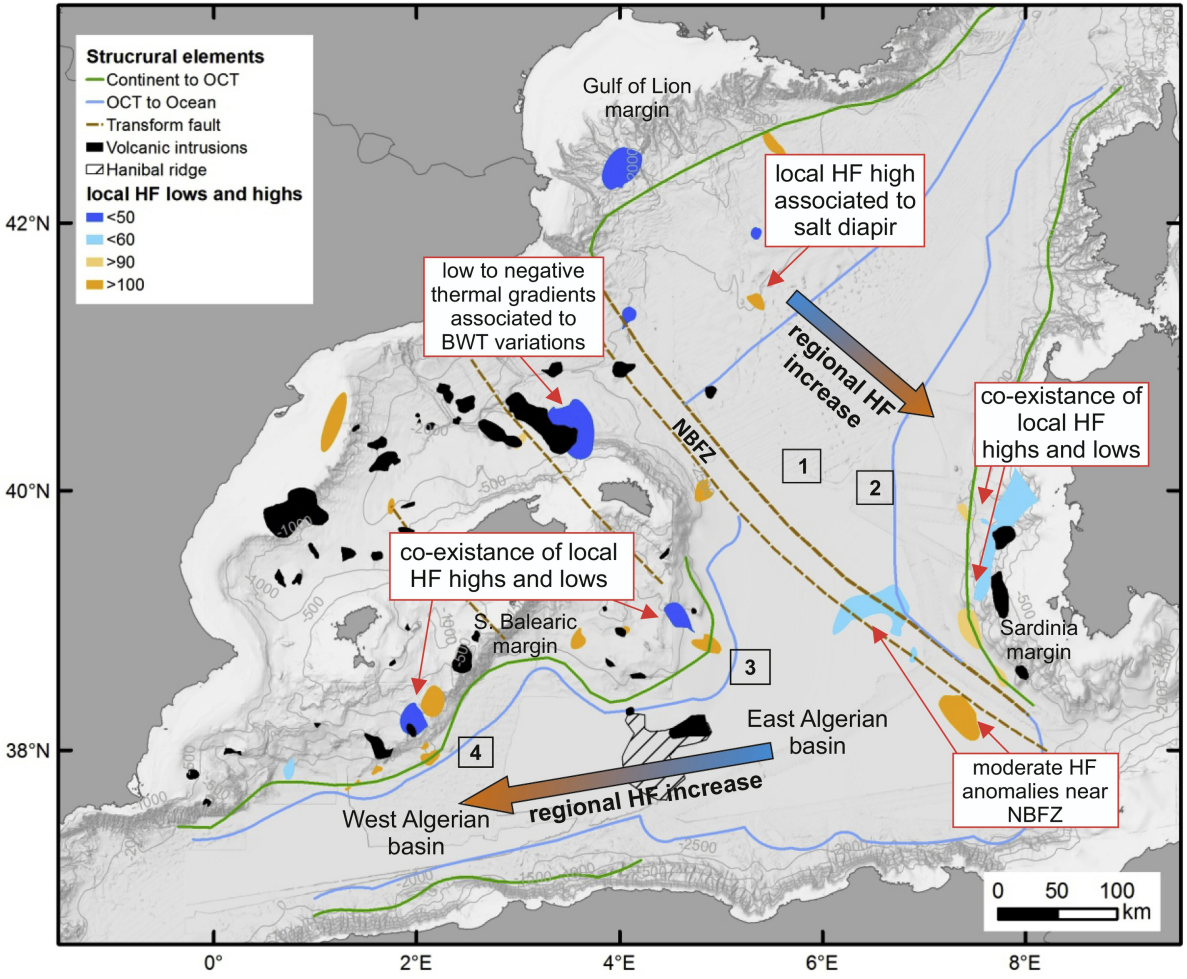
Strucrural elements
Continent to OCT
OCT to Ocean
Transform fault
Volcanic intrusions
Hanibal ridge
local HF lows and highs
<50
<60
>90
>100
Gulf of Lion margin
local HF high associated to salt diapir
low to negative thermal gradients associated to BWT variations
regional HF increase
NBFZ
co-existance of local HF highs and lows
co-existance of local HF highs and lows
S. Balearic margin
Sardinia margin
East Algerian basin
West Algerian basin
regional HF increase
moderate HF anomalies near NBFZ
1
2
3
4
42°N
40°N
38°N
0°
2°E
4°E
6°E
8°E
0 50 100
km

Figure 7

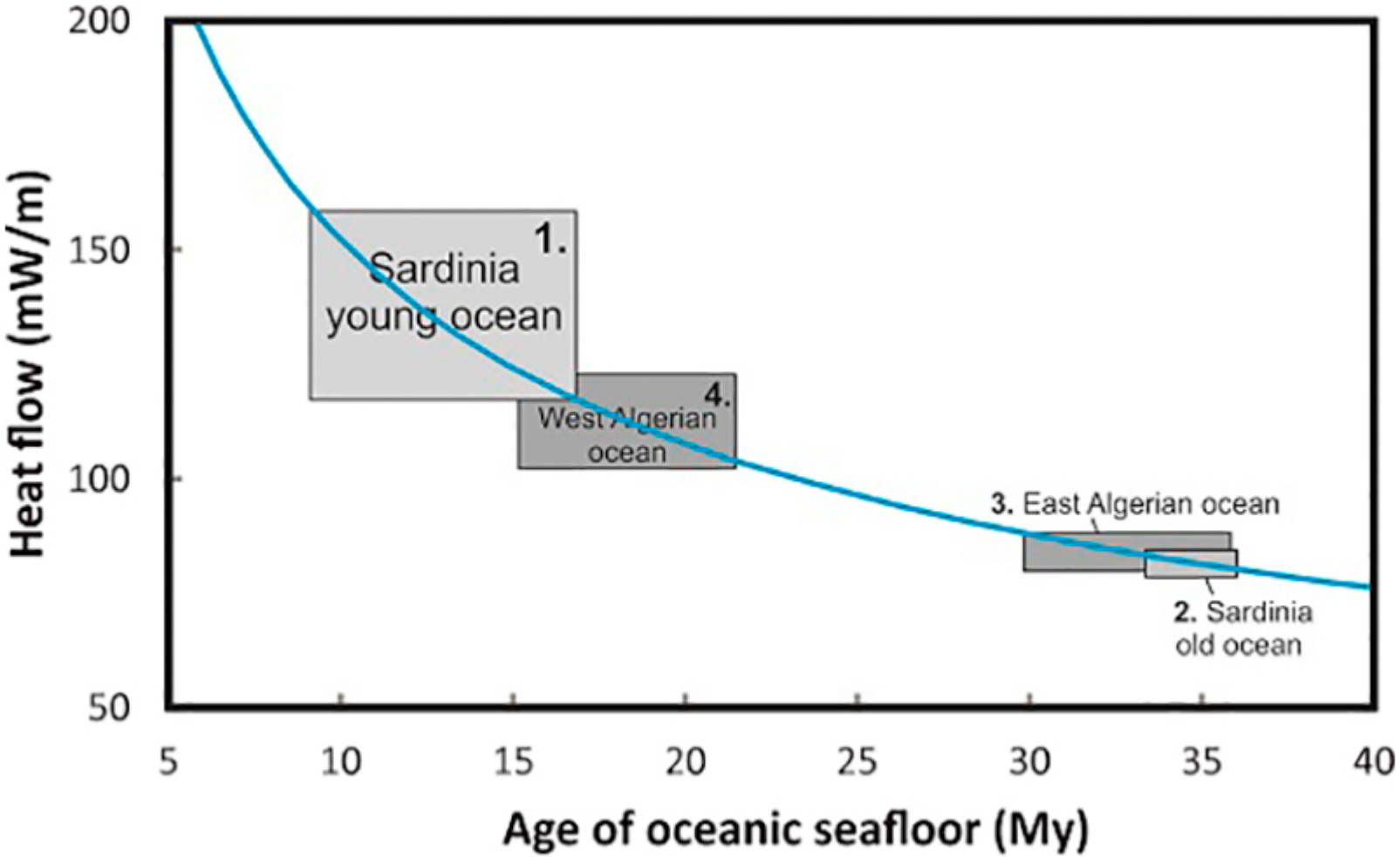
200
150
100
50
Heat flow (mW/m)
1.
Sardinia
young ocean
4.
West Algerian
ocean
3. East Algerian ocean
2. Sardinia
old ocean
5
10
15
20
25
30
35
40
Age of oceanic seafloor (My)

Figure 8